

LASER INTERFEROMETER GRAVITATIONAL WAVE OBSERVATORY
- LIGO -
CALIFORNIA INSTITUTE OF TECHNOLOGY
MASSACHUSETTS INSTITUTE OF TECHNOLOGY

Technical Note **LIGO-T010115- DRAFT- R** 3/21/2001; 10/15/01

**Conceptual Design of the 40 meter Laboratory Upgrade
for prototyping a Advanced LIGO Interferometer**

B. Abbott, G. Billingsley, L. Jones, R. Karwoski, J. Romie, M. Smith, D. Ugolini, S. Vass, A. Weinstein

This is an internal working note
of the LIGO Project.

California Institute of Technology
LIGO Project - MS 18-34
Pasadena CA 91125
Phone (626) 395-2129
Fax (626) 304-9834
E-mail: info@ligo.caltech.edu

Massachusetts Institute of Technology
LIGO Project - MS NW17-161
Cambridge, MA 02139
Phone (617) 253-4824
Fax (617) 253-4824
E-mail: info@ligo.mit.edu

WWW: <http://www.ligo.caltech.edu/>

Conceptual Design of the 40 meter Laboratory Upgrade for prototyping a Advanced LIGO Interferometer

Abstract

We describe the conceptual design for modifications to the Caltech 40 meter Interferometer Laboratory for prototyping Advanced LIGO optical configurations.

Contents

1	Introduction	3
2	Design Requirements	3
2.1	General objectives	3
2.2	Specific requirements and goals	5
3	Advanced LIGO technical innovations tested at the 40m	7
4	Preparation of the 40m laboratory	7
4.1	“LIGO-like” interferometer	8
4.2	Laboratory Infrastructure upgrade	9
4.3	Laboratory hall rehab	9
4.4	Seismic isolation stacks	11
4.5	Bake-out	11
4.6	Vacuum system and controls	12
4.7	New Output Optic Chamber	12
4.8	Mode cleaner	13
4.9	In-vacuum Cables	14
4.10	Optical viewports	14
4.11	Optical tables	15
4.12	Environmental Monitoring	15
4.13	Computing, networking, EPICS and VxWorks	17
4.14	Data Acquisition System	17
4.15	Online Data Monitoring tools	17
4.16	Safety	17
5	Design of optical configuration and control	18
5.1	Design constraints	18
5.2	Optical Configuration	20
5.2.1	Losses and T_{ETM}	20

5.2.2	T_{ITM}	20
5.2.3	T_{PRM} and T_{SRM}	20
5.3	RF sidebands, cavity lengths and control scheme.	21
5.3.1	Mode cleaner	21
5.3.2	Sideband 1, and Power recycling cavity	22
5.3.3	Arms	22
5.3.4	Sideband 2	22
5.3.5	Michelson asymmetry	22
5.3.6	Signal recycling cavity	23
5.3.7	Summary of lengths and frequencies	23
5.3.8	DC detection	25
6	Modeling	25
6.1	Twiddle Model	26
6.2	ModalModel Modeling	29
6.3	End-To-End Modeling	31
6.4	FFT Modeling	32
7	Suspended optical components	34
7.1	Choice of test mass optic size and aspect ratio	34
7.2	Specifications for suspended optics	36
7.3	Radii of curvature	37
7.4	Mode Cleaner optics	38
7.5	Coatings	38
8	Thermal lensing	40
9	Suspensions	41
9.1	Suspension mechanical	41
9.2	Suspension control	42
10	Control Electronics and photoelectronics	42
11	Input mode cleaner	43
12	Optical Layout	47
13	Noise	49
13.1	Fundamental noise at 40m	49
13.2	Sensing noise	50
13.3	Internal thermal noise	50
13.4	Suspension noise	50
13.5	Gas pressure noise	50
13.6	Seismic noise	51
14	Outstanding issues	54
15	Schedule, milestones	54

16 Appendix A - Acronyms	56
17 Appendix B - Gaussian Beam Optics	56
18 Appendix C - RSE, Signal Recycling, Dual Recycling	58
18.1 Motivation	58
18.2 Dual recycling	60
18.3 Coupled cavities	61
18.4 RSE	61
18.5 Initial LIGO, Advanced LIGO, and the 40m	61
19 Acknowledgements	66

1 Introduction

This document summarizes the current thinking on the roles that the Caltech 40m LIGO interferometer (IFO) prototype can play in advanced LIGO R&D, and our current plans on carrying out these roles. Many details and supporting documents can be found on the 40m web page [1].

Serious work on Advanced LIGO design is only just beginning, and the role of the 40m is in as much flux as the Advanced LIGO ideas themselves. Expect that the ideas and designs presented in this document will change in response to the evolving plans for Advanced LIGO.

A 40 Meter Interferometer Technical Advisory Committee exists and has met several times, to aid in formulating the goals of the prototype upgrade. Presentations to this committee are in [2], and minutes of these meetings can be found on the 40m web page [1]. Any and all interested parties are welcome at these meetings, and are also welcome pass on their ideas, comments, criticisms, questions, *etc.*, to the 40m team and the LIGO management.

2 Design Requirements

2.1 General objectives

There are several important reasons to pursue an upgrade/rebuild of the 40m prototype:

- **Optical configurations for Advanced LIGO:** As a test bed or staging area for the design, testing, refinement, and staging of advanced detector configurations anticipated for Advanced LIGO, which require a full IFO for testing. It is anticipated that Advanced LIGO will operate with both power and signal recycling mirrors (dual recycling DR), operated in either the resonant sideband extraction (RSE), signal recycling (SR), or tuned DR configuration. These signal recycling techniques need to be prototyped with a full IFO. This may be regarded as the primary goal of the upgrade, and thus drives its scope.
 - The primary goal of the 40 m upgrade is to demonstrate a control scheme for using resonant sideband extraction (RSE), in either broadband or tuned configuration, appropriate for an optimal LIGO configuration.
 - The purpose of such configurations is to tune the shot-noise limited (high frequency) response of the GW signal. Thus, it may be desirable for the 40m to expose and demonstrate this limit in its noise spectrum. This is *not necessary* if the goal is limited

to establishing a control scheme. For example, even if the GW noise spectrum at the upgraded 40m is dominated by test mass thermal noise, the IFO can still be controlled to the required precision. The predicted transfer function (differential end test mass motion to demodulated optical sensor signal) can be measured directly through excitation of the test masses.

- Note that RSE and DR have been demonstrated at the Garching 30m [3], and at various table-top IFOs [4]. Further, an RSE/DR configuration appropriate for LIGO will be demonstrated at the Glasgow 10m prototype by 2002. Even after these demonstrations, the Advanced LIGO optical control scheme will need a full engineering prototype, using LIGO-engineered sensors and control electronics.
 - The Advanced LIGO optical configuration and control scheme is extremely complex, with many innovations. Without a high-fidelity prototype of the system, it would take excessive time to make the transition from Initial → Advanced LIGO (a mistake learned the hard way during Initial LIGO commissioning). LIGO observatories must remain undisturbed during initial science run, and transition between Initial → Advanced LIGO must proceed as quickly and efficiently as possible. A full engineering prototype is essential for minimizing downtime between Initial → Advanced LIGO; the prototyping pays for itself.
 - The primary goal requires us to test the control scheme with an implementation which resembles as closely as possible the realization to be used in Advanced LIGO. This will minimize the down-time associated with installation of Advanced LIGO in between science runs. This is the primary goal of the 40 m upgrade.
- **Other elements of an advanced LIGO:** The 40m lab can be used as a test bed or staging area for the design, testing, refinement, and staging of other advanced detector elements. Many advanced designs (such as multiple suspensions, advanced seismic isolation, thermal compensation, and advanced thermal noise control) do not require testing on the 40m prototype; they may only require a “table-top” facility or a dedicated facility such as LASTI at MIT, ETF at Stanford, TNI at Caltech, or ARI at Gin Gin, Western Australia. Others (like a delay-line Sagnac IFO, diffractive optics, synchronous recycling, or QND) require such a radical change in the IFO layout that they cannot be accommodated in the available real-estate of the 40m lab. However, many of these innovations may benefit from the use of the 40m prototype. It is therefore useful to rebuild the prototype with the aim of accommodating some of these anticipated developments. These include:
 - multiple pendulum suspensions — this may even be necessary, to extrapolate experience gained at 40m on the electronics/control system to Advanced LIGO. Full scale Advanced LIGO multiple suspensions cannot be accommodated in the existing 40m vacuum chambers.
 - advanced SEI systems — scaled down, of course. The 40m cannot replace full-scale testing at LASTI.
 - Thermal noise measurements with maximized beam width (~flat mirrors) — a big, and challenging, diversion. Mirror Brownian noise will dominate above 100 Hz.
 - LIGO-III: cryogenic TMs, QND, *etc.*

- The 40m lab prototyping complements other facilities, such as the prototyping efforts at MIT and Stanford. The MIT, facility, *e.g.*, is designed for the prototyping of mechanical isolation and suspension systems for advanced LIGO detectors, targeting the low-frequency sensitivity. The 40m focuses on advanced configurations that target the optical sensing noise, which dominates at high frequencies. To summarize:
 - The Caltech 40m will focus on shot (phase, sensing) noise, high- f
 - LASTI at MIT: full-scale SEI, SUS prototyping; low- f
 - TNI at Caltech: thermal noise; middle- f
 - Gingin at Western Australia: high powered lasers, thermal effects
 - ETF at Stanford: Sagnac, high powered lasers
- **Testing of small improvements:** The 40m lab is a facility for the development, testing, implementation, and staging of small improvements to the LIGO interferometers (while they are left undisturbed during science runs), such as new control system hardware or software, variants of the readout control scheme (like third-harmonic sideband control), minor improvements to the suspension mechanics or control, *etc.*. It is far easier for minor modifications to be implemented in the 40m prototype than in the observatory sites.
- **Physicist education/training:** The 40m has been a valuable learning facility for the education of a new generation of GW IFO physicists. The LIGO observatories are largely under the control of operations specialists and engineers, giving inexperienced physicists little opportunity to understand the IFO as a device. The GW IFO community is growing rapidly, and new players need hands-on experience in order to contribute meaningfully to the effort.
- **Public education:** The 40m is a learning facility for the education of the public. The facility should continue to accommodate regularly scheduled tours, and sponsor seminars and educational programs for the science media, teachers, high school students, *etc.*

As noted above, the 40m lab will play a critical role in the development of the Advanced LIGO dual recycling control plant. Its role in the development of advanced suspensions, evaluation of high-power thermal loading, or other aspects of advanced LIGO systems, remains to be determined.

2.2 Specific requirements and goals

In order to achieve the primary objective of providing useful prototyping information for Advanced LIGO, the 40m must, at a minimum satisfy the following requirements:

- The interferometer optical configuration and controls should be designed to emulate, as closely as possible, Advanced LIGO. Any significant deviations from the Advanced LIGO design, due to the smaller vacuum envelope at the 40m, the higher ambient seismic noise, or any reason, should be noted, and its consequences for prototyping the Advanced LIGO optical configuration and controls with high fidelity, understood.
- The interferometer controls, diagnostics, and monitoring must be adequate to the task of bringing and keeping the interferometer in lock, and must be manageable by human operators (section 10).

- The interferometer must be able to be brought into lock (including all length and angular degrees of freedom), with locking times on the order of seconds, and remain robustly in-lock for hours.
- The interferometer must be able to perform stably over significant periods of time, on the order of hours.
- The DC circulating beam power in all cavities, and in all beam frequency components, and at all stages of lock acquisition, should be within expectations from reasonable models (section 6).
- The in-lock GW response function should be measurable, and measured to be within expectations from reasonable models (section 6).
- In particular, the ability to control the degrees of freedom unique to Advanced LIGO (signal recycling cavity length, signal mirror pitch and yaw, peak in response function due to SRC detuning, offset-locking of the arms, DC readout of the L_- degree of freedom, etc) without degrading the control of the Initial LIGO degrees of freedom, should be demonstrated.
- Sources of noise which impact the ability of the interferometer to obtain and maintain lock must be identified, and all efforts must be made to eliminate them.
- Best efforts must be made to reduce those sources of noise that contribute to the GW readout. It is most desirable to be able to expose the shot-noise-limited sensitivity of the interferometer to GWs in the high frequency region (above 1 kHz). (see section 13).
- Systems must be in place to monitor and reduce excess noise from many anticipated sources, including:
 - electrical sources such as pickup (sections 10 and 9.2)
 - scattered light (sections 7 and 12)
 - vacuum pressure (section 4.6)
 - seismic motion (section 4.4)
 - environmental disturbances (section 4.12)
 - suspensions (section 9)
 - suspension controllers (section 9.2)
 - misalignments (sections 6.2 and 10)
 - mode mismatches (section 7).
- All data acquired at the 40m must be logged to frames, and facilities must be available to fully diagnose and characterize IFO performance, on-line and off-line (sections 4.14 and 4.15).
- The laboratory must be a safe environment in which to work, and all laser safety protocols must be established and followed (4.16).

3 Advanced LIGO technical innovations tested at the 40m

Several innovations are anticipated for the Advanced LIGO optical configuration[5]:

- A seventh mirror for signal recycling (length control goes from 4x4 to 5x5 MIMO).
- A detuned signal cavity (carrier off resonance).
- A pair of phase-modulated RF sidebands:
 - frequencies made as low and as high as is practically possible (9/180 MHz for AdvLIGO; 36/180 MHz for 40m).
 - unbalanced: only one sideband in a pair is used.
 - double demodulation to produce error signals.
- A short output mode cleaner to filter out all RF sidebands and higher-order transverse modes.
- Offset-locked arms to allow a controlled amount of arm-filtered carrier light to exit the dark port of BS.
- DC (homodyne) readout of the gravitational wave signal using the arm-filtered carrier light as the local oscillator.

The intention is to prototype the optical configuration with all of these features.

Elements of the optical configuration and controls for Advanced LIGO and the 40m prototype that require further development include:

- Modulators and photodetectors (including wavefront sensors) capable of operating at 180 MHz, with high power beams.
- Double demodulation at 9/180 MHz (AdvLIGO) or 36/180 MHz (40m).
- Servo filter design and optimization.
- An output mode cleaner with controls.
- Arm offset locking control.
- DC demodulation sensor and electronics.

4 Preparation of the 40m laboratory

To support the prototyping of the Advanced LIGO innovations at the 40m, we wish to make the 40m look as LIGO-like as possible, within the obvious constraints associated with the smaller arm length, for several reasons:

- Extrapolating the results of advanced optical configuration R&D from the 40m to LIGO will meet with minimal difficulty and uncertainty.

- The use of LIGO-engineered and tested components (especially the sensors, electronics, monitoring and controls) minimizes the need for extensive re-engineering, and enhances the chances that technical noise will be under control.
- Testing and staging of small modifications to LIGO (such as improved control systems) at the 40m will be most relevant.
- Physicist education and training on the 40m will be most relevant.

4.1 “LIGO-like” interferometer

The anticipated upgrades to make the 40m prototype IFO “LIGO-like” are listed below, along with brief comments to justify them and/or anticipate changes.

Systems in place as of fall 2001 include:

- LIGO-like data acquisition system (DAQS) hardware, disk farm, software, displays.
- LIGO-like EPICS-based detector control system software and displays.
- LIGO-like EPICS-based vacuum control system software and displays.
- LIGO-like environmental monitoring (PEM) hardware, electronics, and software (far fewer PEM devices would be needed at the 40m).
- A LIGO-like 1064 nm pre-stabilized laser (PSL), at LIGO-like power levels of ~ 6 watts at the recycling mirror.

In the next year (AY 2001-2002), it is expected that the control scheme for Advanced LIGO will be finalized, so that the optical and control design of the 40m prototype can also be finalized.

All suspensions and suspended optics, sensing optics and photoelectronics, and control electronics will be assembled during AY 2001-2002, including:

- A suspended mass mode cleaner, so that the optical configuration is as close as possible to Advanced LIGO (to explore interactions between the mode cleaner and the DR IFO), and to provide a stable beam for developing the advanced optical configuration.
- LIGO-like core optical elements (5 mirrors and one beam splitter), with the addition of a seventh (signal recycling) mirror.
- Initial LIGO-like (SOS and scaled-SOS) suspensions and sensors, and digital controllers, for ten suspended optics: three mode cleaner mirrors (MCFM1, MCFM2, and MCFM3), the BS, PRM, and SRM, two ITMs and two ETMs.
- LIGO-like length sensing and control (LSC) photoelectronics, electronics, and software.
- LIGO-like alignment sensing and control (ASC) devices, electronics, and software. This includes the optical lever arms and the WFS sensors and control electronics.

4.2 Laboratory Infrastructure upgrade

By fall 2001, the Laboratory infrastructure upgrade is essentially complete. We limited ourselves to modifications that did not require a rebuild of the building or the vast majority of the vacuum envelope. Essential elements of this work include:

- The dismantling of the old (recycling experiment) IFO, and the distribution of surplus equipment to LIGO and LSC colleagues.
- Enlargement of the IFO hall to make room for optics tables and electronics racks (and for a new 12m input mode cleaner vacuum tube). This required the elimination of the old 40m control room; a new control room was built in the north-west corner of the lab.
- Major building rehabilitation: roof repaired, leaks sealed; new control room and physicist work/lab space; new entrance room/changing area; new paint and wall sealing; new smoke alarms, kill switches, warning lights, *etc.*; rehab of cranes, safety equipment, *etc.*.
- New electrical feeds (with power conditioners) to all electronics racks. One isolation transformer / power conditioner for the PSL, another for all other electronics.
- New EPICS-based vacuum control system, and new or refurbished vacuum equipment (RGA, ion pumps, gate valves, *etc.*). Details on this effort are in [6].
- The installation of a (pre-existing) output optic chamber, the construction and installation of a seismic stack for the output optic chamber, and the design, construction, installation and commissioning of the vacuum envelope for a 12 meter input mode cleaner.
- The development of more flexible, vacuum-compatible cables for the suspension controls and all other in vacuum electronic equipment.
- The seismic noise spectrum at the laboratory was measured during the daytime and the evening, and the transfer functions of the existing 40m test mass chamber seismic stacks were measured. Details are in Ref. [7].
- An active seismic isolation system (STACIS) was procured, installed, and commissioned on all four test mass chambers. Details on this effort are in [8].
- New optical tables and custom support legs for IFO sensing output beams.
- New CDS electronics racks and crates, and new 12" cable trays.
- New computers and networking for IFO DAQS and EPICS monitoring and control, have been procured and set up [9].

4.3 Laboratory hall rehab

The 40m laboratory building underwent a major rehab, beginning July 2000. It was declared complete in March, 2001, and we reverted to clean-room conditions shortly thereafter (we use HEPA filters, but problems remain with the over-pressuring. The lab is effectively a class 10,000 clean room).

Before the work began, the old interferometer was largely dismantled, and the vacuum envelope was protected from harm and dust by covering all optical port glass with hard plastic covers, and the whole vacuum envelope with plastic sheeting.

- The old Argon-based PSL, all old electronics crates and racks, and all cables (except for vacuum and RF) were removed.
- The old PSL, much electronics and green optics, were transferred to Drever’s lab.
- Some electronics were transferred to TNI lab.
- The LIGO-prototype DAQS moved to CDS lab (Wilson house) for DAQ development by Rolf Bork.
- All optical benches (ISC, Oplevs) were disassembled and stored.
- Test masses and suspensions were left in the vacuum chambers (deemed the cleanest and safest place to store them). The recycling mirror went to Saulson’s lab in December 2000. The East Vertex suspension and controllers went to Fred Raab at Hanford, in July 2001. All other green-coated silica optics went to Drever’s Lab.
- We of course keep all useful scopes, analyzers, lasers, oplev optics, SRS amps, etc.

The rehab was managed by Fred Asiri, and much of the construction work was performed by Ray V. Anderson Company (General Contractors) of Los Angeles.

The construction involved many steps:

- Remove the “doghouse” on roof and patch temporarily.
- Re-roof main IFO hall, and North and South Annexes. Caltech contracted Anderson Company to do this in January 2001. The roof held up against the winter rains well.
- We need more space for CDS racks, ISC tables; *etc.*. So, the wall between the old control room and IFO hall was completely removed (leaving posts for supports).
- The under-utilized North Annex became our new office/work space and control room. The north wall of the North Annex building was extended northward to become flush with the north wall of the main IFO hall. A time capsule [10] was buried under the new concrete slab, on 7/31/00.
- The south annex changing area wall was removed, to enlarge that lab space, since the changing area for the south annex will now be shared with the 40m lab.
- The exposed area which had entrances to the 40m lab, north annex, and south annex, was enclosed. It now serves as a common entrance and changing area for the 40m lab, 40m control room, and south annex.
- New electrical wiring was run in the new 40m control room and main IFO hall. New isolation transformers / power conditioners (Topaz XXX) were installed: one for the PSL and one for all other CDS racks. Power lines were run from these transformers, through breaker panels, through kill switches, to the CDS racks in the vertex and end stations.
- New 12” cable trays were installed in the IFO main hall, for ISC and CDS.
- New floor tiles, cieling tiles, paint, wall sealing, window sealing, door sealing, etc.

The changes to the layout of the laboratory are illustrated in Fig. 1.

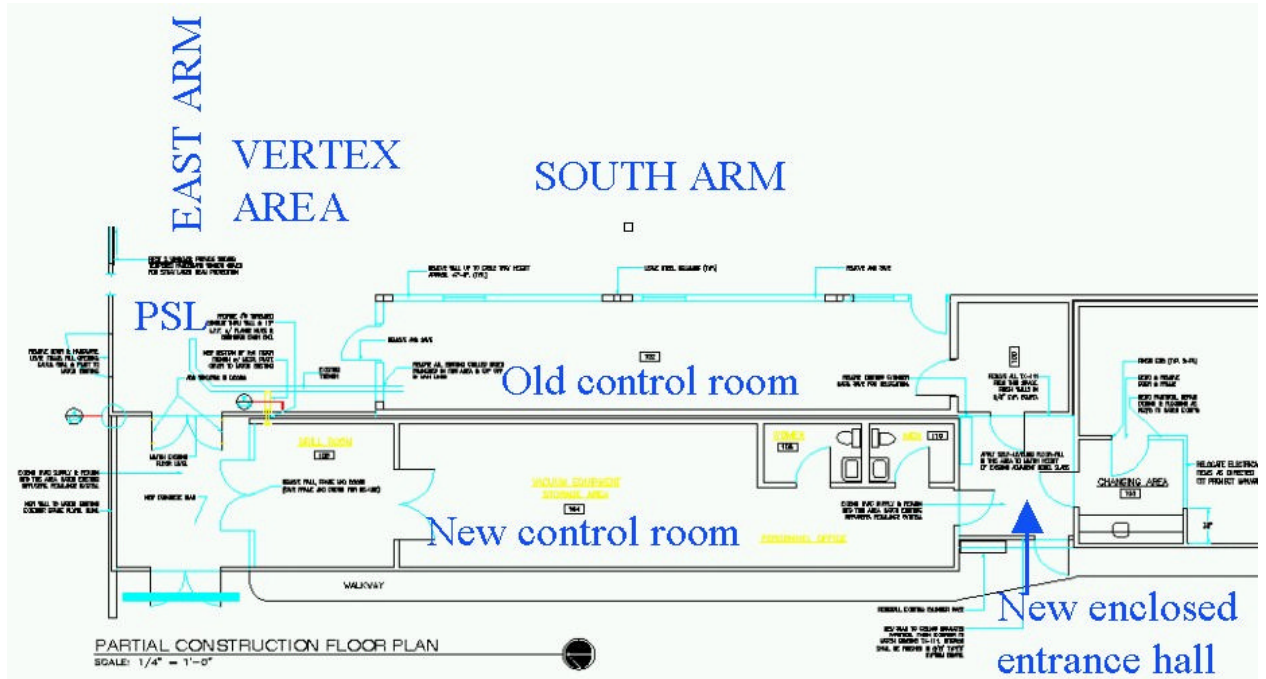


Figure 1: Illustration of the modifications made to the layout of the 40m laboratory.

4.4 Seismic isolation stacks

The current seismic isolation stacks in the test mass chambers on the 40m were prototypes for LIGO HAM stacks [11, 12, 13, 14]. They are fully functional, providing effective passive isolation from seismic noise above 100 Hz, using viton springs [7]. The LIGO I passive seismic isolation stacks use damped-metal springs which are somewhat softer (but less well damped), provide effective isolation above 40 Hz (but potentially worse total rms motion due to inadequately damped resonant peaks below 10 Hz). The active system proposed for Advanced LIGO is effective at 10 Hz or below.

We considered rebuilding the 40m stacks with damped-metal springs (we even purchased the springs). In the end, we decided that the improved noise at high frequencies was not worth the cost of degraded total rms motion and its (uncertain) impact on the control system (lock acquisition). This is documented in [15].

To help reduce the rms motion of the mirrors as an aid to lock acquisition in the noisier seismic environment of the 40m lab (as compared with the sites), we installed active seismic isolation systems on all four test mass chambers. The devices are commercial versions of the prototype Barry Controls active isolators used in the PNI experiment at MIT [16]. These devices work acceptably, and their performance is documented in Ref. [8].

4.5 Bake-out

The presence of fluorocarbons in the 40m RGA suggests that the existing viton springs in the passive seismic stacks are contaminating the vacuum. We initially planned to disassemble, and bake and clean, the existing stacks. We planned to bake out the 40m beam tubes and pumps, which would require raising the entire interferometer vacuum envelope in order to apply heat to the bottoms of the chambers.

However, the level of fluorocarbons in the 40m RGA is not very high, and there is no evidence that such contaminants cause problems with IR laser light [17].

After reviewing the pros and cons [15], we decided that a stack rebuild and vacuum envelope bakeout was of questionable value and required great effort and expense; it was abandoned.

All newly constructed elements of the vacuum envelope and in-vacuum IFO components will, of course, be cleaned and baked in accordance with standard LIGO procedures.

4.6 Vacuum system and controls

The vacuum envelope, instrumentation, and EPICS-based control system for the 40m IFO is complete. As mentioned above, the new output optic chamber, 12m mode cleaner tube and MCCM chamber, and active seismic isolation, have been installed. As of Fall 2001, several large items remain to be installed: two seismic stacks, cables, and all IFO components. All these in-vacuum components are or will be cleaned, baked, and RGA scanned prior to installation in the vacuum envelope.

The vacuum envelope is instrumented with three molecular turbopumps, four ion pumps, and one cryopump (as well as 4 roughing pumps). Pirani and cold cathode vacuum gauges are distributed about all the vacuum lines, and in the main vacuum envelope. Two RGAs are installed for simultaneous use: a Dycor M200MC and an SRS RGA200. Several calibrated leaks are available.

During normal IFO operation, only the one maglev turbopump and the four ion pumps would be operating; the others create lots of mechanical noise and should not be necessary. The total pressure under those conditions is below 10^{-6} torr, dominated by atmospheric gases (in order of partial pressures: H_2O , N_2 , O_2 , H_2 , Ar, CO_2 , Ne). Hydrocarbons (from pump oil) with AMU's of 41, 51, 55, 64, 67, 78, *etc.*, are typically below 10^{-11} torr and are carefully monitored.

It is believed that such hydrocarbon levels do not present a hazard to the high-quality optics in the presence of the high IR laser powers. The total pressure contributes little to the phase noise in the GW channel; see section 13.

It is possible that the vacuum may degrade due to the presence of equipment yet to be installed. It may also be necessary to improve the vacuum in order to further reduce phase noise or contamination of IFO components. If necessary, it is possible to further improve the vacuum by installing additional pumps and diagnostic equipment.

The new EPICS-based vacuum monitoring and control system works well and reliably, and is easy to use. Several software interlocks back up and complement the required hardware interlocks. Vacuum data are continuously logged to disk in frames by the DAQS system. Second trends are available on disk with a one month look-back, and minute trends are available with a 150 day look-back (which will be archived).

4.7 New Output Optic Chamber

Two “side chambers” with seismic isolation (one-leg masses, viton springs, 4 stages if you include the top table) were built for the 40m Mark II interferometer.

One has been in use for many years as the “input optic chamber”, housing the faraday isolator, RF modulator, and mode matching telescope.

In the Advanced LIGO prototype, RF modulators will be on the PSL table (in air). The input optic chamber will house two of the three 12m suspended mass mode cleaner optics, the faraday isolator, and a mode matching telescope.

The second “output optic” chamber will house a small, monolithic output mode cleaner, as described in section 5.3.8, and will provide paths for the input beam and for many output beams.

This output optic chamber (OOC) has been pumped on for some months and is clean enough to be installed in the 40m vacuum without baking [18].

The OOC was installed and commissioned for the first time in July 2001, along with a new 29.5” adjustable bellows spool piece that connects it to the input optic chamber (IOC). A new seismic isolation stack (almost identical to the input side chamber stack, but with some small changes to correct some errors in the original design) was constructed and cleaned, and will be installed as soon as in-vacuum cables are available (late fall 2001).

4.8 Mode cleaner

A long suspended-mass mode cleaner would deliver a laser beam with LIGO-like beam quality (low frequency noise, low amplitude noise, low higher order mode HOM power, and low beam position and pointing jitter); this presumably will make lock acquisition and IFO operation less difficult and more LIGO-like, and increase the chances that fundamental noise sources can be exposed. (On the other hand, previous experiments at the 40m have found that the noise floor has not been seen to be limited by frequency noise, pointing jitter or HOM losses).

The current 40m has a fixed mirror (514 nm light) mode cleaner in a 1m quartz tube, suspended from beampipe on springs. It is used to further stabilize the PSL frequency.

The current 40m configuration places the RF modulator pockels cell *after* the mode cleaner, so that the mode cleaner is not required to pass the sidebands. This simplifies the requirements on the mode cleaner considerably (LIGO needs a 12 meter MC to pass the sidebands). However, all the noise generated in the Pockels cell goes right into the IFO.

Further, the pockels cell is in vacuum; the heat load and inaccessibility has led to numerous heat-related failures. If the pockels cell can be placed on the PSL table before the vacuum system and mode cleaner, that will help a lot; but it requires a long mode cleaner to pass the RF sidebands.

For control realism, we would like to have an input mode cleaner that is as similar to what is envisioned for Advanced LIGO as possible. Current thought is that an Advanced LIGO input mode cleaner could look very similar to the Initial LIGO 12m mode cleaner; it might be increased to 16.7m in half-length in order to pass 9 MHz RF sidebands for control. As discussed in section 5.3, the 40m will operate with ~ 36 MHz sidebands, and a 12.7m mode cleaner is called for.

These considerations have led to a decision to construct a 12.7m suspended mass input mode cleaner for the 40m. A triangular 12m suspended-mass mode cleaner was designed for the 40m back in 1995, was partially built but never installed, and was subsequently disassembled. We have recovered three 4m long beam pipes, an end mirror chamber and seismic stack, and supports.

We have designed, constructed, and installed the additional hardware required to assemble the 12m input mode cleaner vacuum envelope. The vacuum equipment was cleaned and baked, and installed in the 40m vacuum envelope in the July of 2001. The entire 40m vacuum envelope, including the new output optic chamber, the 12m mode cleaner beam tube, and the mode cleaner curved mirror end chamber, was pumped down in early August; the vacuum pressure reached pre-installation levels shortly thereafter, with no indication (from RGA scans) of contamination. The system was leak checked successfully.

The input mode cleaner design is described in section 11. The plan is to install the optical components as soon as the optics are ready, in winter 2002.

4.9 In-vacuum Cables

The flat-ribbon 25-conductor kapton-insulated in-vacuum cables were considered for use in the 40m. However, our seismic stacks are much smaller than LIGO's; these cables are rather stiff, and there was some concern that they could mechanically short the seismic stacks, especially the small stack in the mode cleaner curved mirror chamber. Further, there is very little room between the stacks and the chamber walls, making it very difficult to run the cables from the optical table down the stacks to the vacuum feedthrough.

In addition, the CDS group would prefer twisted-pair cables, with a braided shielding around a bundle of 12-twisted-pairs.

We therefore searched for a flexible, small diameter vacuum-compatible wire which could be formed into 12 twisted-pairs with braided shielding. After some searching and prototyping, we arrived at a satisfactory solution, using Cooner wire (as is used for the OSEM pigtails). Cooner will twist the wires and braid the shielding to our specs (12 twisted pair, 5 tpi, of 65/46ga with 0.005" FEP jacket; braided shield of 24X7/38ga, copper, 90% coverage). These cables are made of materials that are vacuum approved for the LIGO sites (and, in fact, are in use there).

We require approximately 35 such cables, each 8 feet long, to service 10 suspended optics (2 cables per optic), along with miscellaneous low-voltage electronic devices (two pairs of steering mirrors, mode-matching telescope, beam flags, output mode cleaner PZT, an in-vacuum DC photodetector, and spares).

In addition, we require cable clamps and associated hardware for routing the cables down the stacks, and vacuum feedthroughs. All these parts will be in hand by December of 2001. They will be cleaned and baked. We plan to install the cables in February 2002. At that time, we will also install the new seismic stacks in the output optic chamber and the mode cleaner end chamber. At that point, the vacuum envelope will be 100% complete.

4.10 Optical viewports

The 40m vacuum system contained many optical windows to permit the entrance and exit of the main Argon laser beam, of the optical lever He:Ne beams, of camera viewports, and visual access. These windows were specially coated to minimize reflection of the green laser light.

We are replacing all optical viewports on the 40m vacuum envelope with new, or newly coated, windows. All viewports attach to 8" cf vacuum flanges. These fall into several categories:

- New optical-quality (BK-7) windows, AR coated for 1064 nm. One for the input beam and one for the (several) exit beams in the vertex area. The coated windows are purchased from Cascade Optical. They should reduce reflection to $< 0.2\%$ at normal incidence for 1064 light. These mount onto newly-designed viewport seal flanges which will hold the window at a 2.5degree tilt, to minimize backscatter into the IFO. These flanges are being built by CES at Caltech. Mike Smith has done detailed BRDF calculations of the backscattering, and concludes that 2.5degrees is sufficient, even for the ETM transmitted beams (which are the worst case).
- New optical-quality (BK-7) windows, AR coated for broad-band. They will be used for the pick-off beams, and for ETMx and ETMy beams. These windows will also have optical lever beams, which is why they will be AR coated for broad-band. The broad-band coating should reduce reflection to $< 0.75\%$ for both 1064 and red He:Ne light.

- 12 “camera”-quality optical viewports (7056 glass), welded onto flanges, already existed at the 40m laboratory. They were AR-coated for 1064 by Cascade optical. These will be used for all the camera viewports and other viewports for visual access.

4.11 Optical tables

We require high quality optical tables and table supports for the input beam (PSL) and all output beams. We have re-used the 6’x10’ Newport 2000 optical table that was used for the laser in the Mark II 40m experiments. All other tables are newly acquired, (TMC CleanTop II 790 series), and are supported by legs that were specially designed and constructed to maximize stability and minimize resonances. All tables will be permanently installed by the end of October 2001.

The tables at the laboratory, their dimensions and locations, and the beams that they are intended to sense, are as follows:

- ETMX (2’x4’, 4” thick, 32.75” high) (just east of east end) - East arm transmitted, initial pointing
- ETMY (2’x4’, 4” thick, 32.75” high) (just south of south end) - South arm transmitted
- OPLEV (2’x4’, 4” thick, 32.75” high) (just north of vertex) - optical levers for vertex suspensions
- AP2 (3’x4’, 12” thick, 32.75” high) (just west of vertex) - OMC transmitted, and beam output mirrors
- BSPO (3’x5’, 12” thick, 31.25” high) (just south of vertex) - BS pickoff beam
- ITMXY (3’x5’, 12” thick, 32.75” high) (just east of vertex) - ITMX, ITMY pickoff beams
- AP1 (4’x6’, 12” thick, 32.75” high) (south of PSL and SP&MC tables) -
- SP&MC (5’x12’, 24” thick, 32.75” high) (just south of PSL table)
- PSL (5’x10’, 12” thick, 25” high)

All beams are nominally 36.75” from the floor, except for the ones on the PSL table.

All ISC table tops are nominally 32.75” from the floor, EXCEPT for the BSPO table, which must fit below the MC beam tube. The beam height is 4” from table top.

The PSL table top is 25” from floor, and the beam height is 3” from table top. A periscope will bring the beam from 25+3” to 36.75”.

The vacuum chamber tables are nominally 31.25” from the floor, and the beam height is 5.5” from table top.

The locations of the vacuum chambers and tables in the vertex area are shown in Fig. 2.

4.12 Environmental Monitoring

It is *presumed* that a physical environment monitoring (PEM) system similar in design (but much scaled back in scope) will be sufficient for identifying and reducing the effect of environmental disturbances that negatively impact the ability of the IFO to acquire or maintain lock, or find their way into the GW readout channel(s).

As of Fall 2001, the following devices have been installed or will soon be installed in the DAQS and/or EPICS systems:

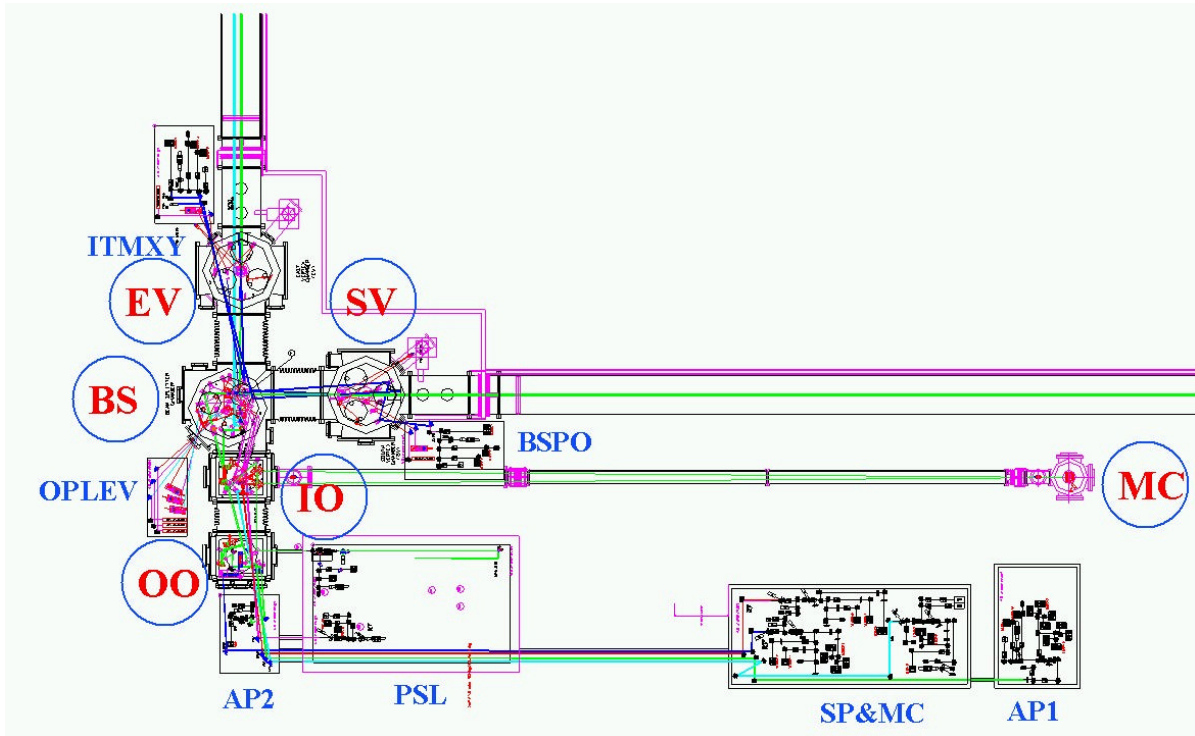


Figure 2: Illustration of the locations of the vacuum chambers and tables in the vertex area of the 40m laboratory.

- Dust particle count at 1.0 and 0.5 μm diameters, with a MetOne 227.
- Inside and outside weather conditions (temperature, humidity, barometric pressure, rain, wind speed and direction) using a Davis Instruments 7440 Deluxe Indoor/Outdoor Station with WeatherLink.
- Two three-axis accelerometers (Wilcoxon 731A).
- A one-axis (vertical) seismometer (Kinometrics Ranger SS-1).
- Vacuum pressures and RGA partial pressures.

Devices that we anticipate installing within the next 6 months:

- Readout of the STACIS controllers.
- microphones.
- Magnetometer.
- Power line monitor.
- RF monitor.

We will require help from knowledgeable LIGO personnel for choosing appropriate and economical solutions for these devices.

4.13 Computing, networking, EPICS and VxWorks

Currently, the CDS group believes that the architecture of the control, monitoring and data systems used in Initial LIGO (embedded VME processors running VxWorks and EPICS, and reflective memory modules with fiber links for the fast control, DAQS, and monitoring networks) will be adequate for Advanced LIGO as well. Thus, the 40m lab will be outfitted with a full complement of these control devices.

The lab will have the infrastructure for maintaining all the embedded processors required for prototyping AdvLIGO, including fiber links to the “end stations” 40 meters away.

Currently, the 40m lab has a small number of embedded VME processors running VxWorks and EPICS, as at the sites. As of Fall 2001, we have a DAQS system with a fiber-based reflective memory network; three “IOCs” (I/O controllers) controlling the vacuum, PSL, and the PEM systems; an “EDCU” (Electronic Data Collection Unit) for passing the slow EPICS channels into the DAQS; and a 64-channel “ADCU” (Analog Data Collection Unit) for the fast PSL and PEM signals.

We have a Sun Ultra 60 serving as a DAQS frame builder (fb40m). We will shortly have a Sun Ultra 30 serving as a Frame Broadcaster (br40m), driving a dedicated “Frame Broadcasting” network (100BT) connected to a Sun Blade 100 workstation running DMT (dmt140m). We have two Sun Blade 100 workstations (op140m, op240m) to serve as operator consoles.

We currently have a “martian” network (131.215.113.xxx) isolated from the Caltech net through a gateway (rana). All the VME processors, Sun computers, and several PCs, are on this martian network.

In order to archive our data (frame files), we require a fast fiber link to the CACR archive. Albert Lazzarini and Larry Wallace are arranging for this, and we hope to have it in place by 1Q02.

4.14 Data Acquisition System

The data acquisition system (DAQS) for Initial LIGO was prototyped at the 40m by Rolf Bork and company. It served the 40m IFO until it was removed for upgrade in summer 2000.

In spring 2001, the hardware and software for the upgraded DAQS was installed in the 40m lab, including a Sun Ultra 60 framebuilder, a DAQS crate with a pentium VME processor, a 600 GB RAID array, a 64-channel “ADCU” (Analog Data Collection Unit) for fast signals, and DataView software.

Except for failures of the RAID array disks (which have been replaced), this system has been in continuous and reliable use since April 2001.

4.15 Online Data Monitoring tools

We are currently developing and installing a full complement of online software, including site-specific EPICS summary screens, Data Monitoring (DMT) software, DTT, LIGOTools, *etc.*

We do not currently foresee the need for an LDAS installation at the 40m lab. This may change!

4.16 Safety

The entire 40m IFO hall is a Laser Hazard Area, governed by an approved Standard Operating Procedure [19] adhering to the overall LIGO laser safety plan [20]. The 40m Laboratory Safety Officers are Steve Vass and Dennis Ugolini.

In addition to the Initial LIGO 10-watt laser, the laboratory will operate approximately 10 class IIIa He:Ne lasers operating at 635 nm (red) at less than 5 mW, used as optical levers for sensing the alignment of the suspended optics in the IFO.

There are three hazard conditions: Laser Safe (10 W laser interlock is off, so that the laser is not capable of being powered), Laser Hazard (laser interlock is on so that the laser is capable of being powered), and Laser Hazard - Doors Open (laser interlock is on so that the laser is capable of being powered, and the PSL enclosure doors are open). Procedures for safely transiting between states are outlined in [19].

During normal operations, all effort is made to keep the PSL enclosure doors closed; and when open, special care is required for all people working near the PSL enclosure. At the moment, the enclosure doors are not properly sensing their state (open/closed); this will be fixed soon.

No one should energize or work with or near the 40m IFO LIGO 10-W Laser unless authorized to do so. All persons operating the laser must have completed laser safety training and be registered with the LIGO Laboratory as specified in LIGO-M960001-B-P. All persons operating the laser must be familiar with all operating procedures, including emergency service procedures, emergency phone numbers, etc. The Responsible Laser Operator shall coordinate activities on or in the vicinity of the laser optical table.

All entrances to the Laser Hazard Area are clearly marked with placards and lighted warning signs, and all personnel must wear protective laser goggles (optical density of 5.0 or greater for 1064) in that area when the Laser Hazard conditions apply. A supply of such goggles are available at the main entrance to the Laser Hazard Area. Laser kill switches (which cause automatic transition to the Laser Safe condition) are located in several places around the lab, near the PSL enclosure, and at all entrances.

5 Design of optical configuration and control

The design of the 40m prototype IFO upgrade is based on the “straw-man” optical configuration and control design outlined at the August 2000 LSC meeting by Peter Fritschel and Ken Strain [21], shown schematically in Fig. 3. Further detail can be found in the Advanced LIGO technical notes [5].

Considerable work must go in to understanding and optimizing this design, and that work is only just beginning. Expect that the ideas and designs presented in this document will change in response to the evolving plans for Advanced LIGO.

However, the overall optical and controls design seems rather robust. If no radical changes are introduced, there is sufficient information to do a detailed design of a high-fidelity 40m prototype. This is described in the following sections.

5.1 Design constraints

Some of the constraints and considerations that guide our design are given below:

- We want to determine the configuration for Advanced LIGO and the 40m simultaneously (same modeling tools, such as matlab, twiddle, and e2e files) to make sure they are similar, and that differences are understood.
- The optical configuration design (mirror reflectances, *etc.*) are chosen to be the same as current Advanced LIGO II design. This means that all cavity finesses are designed to be the

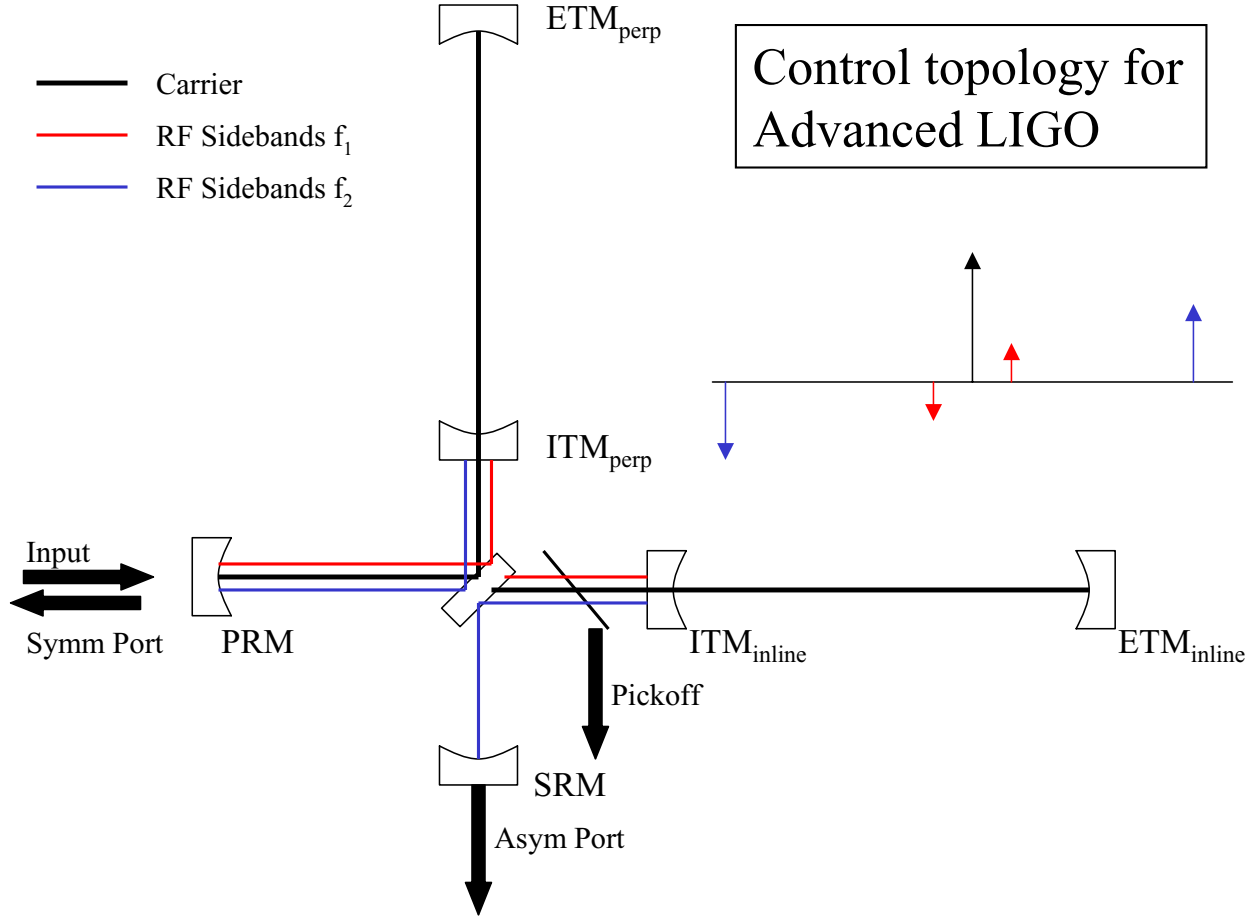


Figure 3: Schematic of the control topology of Advanced LIGO (and the 40m upgrade), showing the pattern which laser light components (carrier, RF sidebands) resonant in the various optical cavities, and the ports at which the control signals are sensed.

same. Since the 40m has much shorter arms, the cavity storage times and frequency responses will thus be very different. For example, the arm cavity pole for a 4 km cavity with 0.5% transmitting ITMs is 15 Hz, while for 40 m arms it is at 1500 Hz. Any attempt to match the arm cavity pole / storage time will require exceedingly high finesse for the 40m arms, making lock acquisition and control very difficult. We judge that the prototype will achieve higher fidelity to Advanced LIGO, from the controls perspective, by matching finesse, not pole frequency.

- Because of the shorter arm length, the detuning of the signal recycling cavity (SRC) will be different: for Advanced LIGO, the SRC will be detuned by $0.038\pi/2$ (one-way phase advance) in the direction of broadening the bandwidth beyond the arm cavity pole of 15 Hz out to ~ 300 Hz (RSE); for the 40m, we plan to detune the SRC by $0.237\pi/2$ to bring the bandwidth from the cavity pole of 1500 Hz out to 4000 Hz. The control of the IFO has very little dependence on the detune phase; from the perspective of the IFO control, the direction and amount of detuning doesn't matter. Thus, a test of detuning at the 40m will be directly relevant for Advanced LIGO. As a purely practical matter, the larger tune phase employed

at the 40m makes the beam-splitter chamber somewhat less congested, and it puts the dip in the sensitivity curve out to a high enough frequency that it can be detected over the reduced test mass thermal noise.

- Because of shorter vacuum envelope, the choice of cavity lengths, RF frequencies, *etc.*, will be different. We can make the control scheme very close to that of Advanced LIGO, and err on the side of a somewhat less robust (diagonal) control matrix.
- The beam spot sizes, mirror ROCs, will of course be different as well, by a factor $\sqrt{4000/400} = 10$. In the first round of experiments, we will not attempt to blow up the beam sizes by using a less stable arm cavity (as is envisioned for Advanced LIGO). New core optics would be required if we choose to do this in the future.
- The input mode cleaner will be almost identical to Initial LIGO, which is similar to the input mode cleaner envisioned for Advanced LIGO.
- We don't know what the output mode cleaner for Advanced LIGO will look like; however, we are designing a short monolithic output mode cleaner for the 40m (almost identical to the PSL PMC), which could easily be used in Advanced LIGO (if a rigid, short, OMC is consistent with the design, and if a scheme can be developed to suspend it).

5.2 Optical Configuration

5.2.1 Losses and T_{ETM}

Mirror coating and substrate losses drive many aspects of the IFO optical design. Expectations for these values with sapphire optics are still under study. For definiteness, we take middle-ish expectations for the fused silica optics and coatings realized for Initial LIGO:

- Absorption and scattering losses in all optics: 37.5 ppm.
- Absorption, scattering, pickoff losses in transmissive optics in the PRC (BS, ITM substrates) add up to 1000 ppm.
- ETM transmissivity of $T_{ETM} = 10$ ppm to let some light out for monitoring and lock acquisition. This loss is *included* in the 37.5 ppm loss assumed above.

5.2.2 T_{ITM}

The optimization of the dual-recycled Advanced LIGO for binary inspirals was performed by Ken Strain [21], using the BENCH package [22]. He concluded that for both sapphire and fused silica test masses, high(er) finesse arms are desired: $T_{ITM} = 0.005$, leading to finesse = 1231; $G_{arm} = 770$; $f_{armpole} = 15$ Hz (LIGO), 1591 Hz (40 m). (Initial LIGO has $T_{ITM} = 0.03$).

5.2.3 T_{PRM} and T_{SRM}

We choose the transmissivity of the power recycling mirror T_{PRM} to let 1% of carrier light power be reflected at the symmetric port. With the loss assumptions given above, this gives $T_{PRM} = 0.086$; PRC finesse = 38; $G_{PRC} = 14$ (depends on losses!). These numbers will be the same for Advanced LIGO and the 40m.

The peak detuned response of the signal recycling cavity (SRC) for Advanced LIGO was optimized by Ken Strain, as noted above. A near-optimal response was obtained with a peak detune frequency of $\simeq 330$ Hz and signal recycling mirror transmittance $T_{SRM} = 0.05$. We choose the same T_{SRM} for 40m as for Advanced LIGO, so as to obtain the same SRC finesse.

We cannot hope to achieve the same peak frequency due to the much shorter arms of the 40m; we aim for a peak frequency of $\simeq 4000$ Hz. This may change as the Advanced LIGO design is further optimized.

5.3 RF sidebands, cavity lengths and control scheme.

An earlier version of this discussion of the 40m optical configuration, appropriate for a broadband RSE configuration, is in Ref. [23].

There will be two pairs of phase-modulated sidebands, placed on the main beam just downstream of the PSL, in air, using two fast- and high-powered Pockels cells in series. Since these are in series, the second Pockels cell will place sidebands on the first pair of sidebands, producing four desired sidebands at $(\pm f_1, \pm f_2)$ and four “parasitic” sidebands at $(\pm f_1 \pm f_2)$ (plus higher orders).

The goal is to measure and control the arm degrees of freedom (L_+ and L_-) using beats between the carrier and one of the two pairs of sidebands, and the power- and signal-recycled Michelson degrees of freedom (l_+ , l_- , and l_s) using beats between the pairs of sidebands. No carrier light is used to sense these “short” degrees of freedom, so that their signals are not swamped by the large signals from the high-finesse long arms.

The Michelson asymmetry is set to be a bright port for the higher of the two RF sidebands (f_2). The lower RF sideband (f_1) should be as low as possible, so that f_2 “sees” the signal mirror while f_1 does not, providing maximal separation between l_+ and l_s .

Because the 40m cannot accommodate a large power recycling cavity (PRC) (it is limited by the vacuum envelope to be on the order of 2 meters), we will see that the 40m cannot make use of values for f_1 as low as that proposed for Advanced LIGO (9 MHz); thus, the ratio f_1/f_2 will be larger at the 40m than at LIGO and the separation between l_+ and l_s will be worse. If we can make this work at the 40m, it will only be easier at LIGO (I think).

Both pairs of sidebands will be placed on the beam before the input mode cleaner. The mode cleaner must pass both pairs of sidebands, so their frequencies must be chosen to be multiples of the FSR of the mode cleaner.

The “detuning” of the signal recycling cavity (SRC, discussed below) results in an imbalance between the two sidebands in a phase-modulated pair. (In Initial LIGO, the RF sidebands have a balanced response in the IFO). The upper and lower sidebands will experience different buildup in the PRC and SRC, and different reflectivities and transmittances through the IFO. This imbalancing has both positive and negative consequences; but the control scheme discussed below is far less robust with balanced sidebands (as in broadband RSE or signal recycling). Fortunately, it is anticipated that Advanced LIGO will always operate with a detuned signal recycling cavity.

5.3.1 Mode cleaner

The input mode cleaner will have a half-length of $L_{MC} = 13.542$ m, determined by the length of the 8” diameter and 12 m long MC pipe, and the positions of the suspensions in the chambers on either end of the pipe. Then, $\text{FSR}_{MC} = c/2L_{MC} = 11.069$ MHz. For a triangular mode cleaner, it’s the *half*-length, and not the total length, which determines the FSR (for a linear Fabry-Perot

cavity, the round-trip length is twice the total length; for a triangular Fabry-Perot, the total round trip length is twice the half length).

5.3.2 Sideband 1, and Power recycling cavity

The f_1 sidebands must resonate in the MC, so they must be an integral multiple of the free spectral range of the mode cleaner $FSR_{MC} = c/2L_{MC}$: $f_1 = n_1 FSR_{MC}$, where n_1 is some integer.

In addition, they must resonate in the PRC. Recall that the carrier sees an overcoupled arm reflectivity whose sign is opposite to that of the sidebands. Thus, if the carrier is resonant in the PRC, the sidebands must experience an additional phase shift of $(2n_2 + 1)\pi$, where n_2 is some integer. Thus, we require $f_1 = (2n_2 + 1)c/(4L_{PRC})$. The length of the PRC can be made as short as 2 m or as long as 2.5 m or maybe even longer. We want f_1 to be as small as possible (see above), so we choose $n_2 = 0$ and thus $f_1 = c/(4L_{PRC})$. The smallest multiple of FSR_{MC} that can satisfy this is $n_1 = 3$, and $f_1 = 3FSR_{MC} = 33.207$ MHz, with $L_{PRC} = c/(4f_1) = 2.257$ m.

5.3.3 Arms

The f_1 sidebands should not be resonant in the arm cavities. They should avoid exact anti-resonance, because then their even harmonics will be resonant in the arms. The arm cavity finesse is so high that even a slight departure from exact resonance will lead to very little sideband light in the arms (as desired). However, separation of the length degrees of freedom is best when the f_1 and f_2 sidebands are both pretty close to anti-resonance, so that negligible sideband light enters the arm cavities. Thus, we require $L_{arm} = (n_3 + 1/2)c/(2f_1)$ with n_3 close to an integer (but not exactly an integer, so that even harmonics will not be resonant in the arms). With $L_{arm} = 38.55$ m, we get $n_3 = 8.04$.

5.3.4 Sideband 2

Now we want the second pair of sidebands (f_2) to be as high as possible, and resonant in the MC and in the PRC; so it should be an multiple of f_1 : $f_2 = n_4 f_1 = n_4 n_1 FSR_{MC}$. We can choose $n_1 = 3$ and $n_4 = 5$, so that $f_2 = 5f_1 = 15FSR_{MC} = 166.033$ MHz. We will need to demodulate at $f_1 + f_2 = 200$ MHz, which is close to the $180 + 9$ MHz chosen for Advanced LIGO. It's about as high as one dares to go using present photodetector, mixer, and RF distribution technology.

As we will see below, the mixer will need to demodulate at $f_2 \pm f_1$; at Advanced LIGO, this is $180+9 = 189$ MHz; but at the 40m, this is 200 MHz. Too high? Actually, the current scheme calls for *double-demodulation*; instead of demodulating at $f_2 + f_1$ and at $f_2 - f_1$, one can demodulate at f_2 , and then feed the output to a mixer demodulating at f_1 ; this accomplishes the same thing. So we'll only need to demodulate at 165 MHz at the 40m.

5.3.5 Michelson asymmetry

Now we choose the Michelson asymmetry to make the asymmetric port of the BS "bright" for the f_2 sidebands, so that the f_2 sidebands "see" the signal recycling mirror. We need a Michelson asymmetry of $\delta l = c/(4f_2) = 0.451$ m, or Michelson arm lengths that differ by ± 0.251 m. This is relatively easy to arrange in the 40m vacuum envelope.

Of course, some of the f_1 sidebands will also go out the asymmetric port of the BS. Because f_1/f_2 must be larger at the 40m than at LIGO, more f_1 sideband will go out the asymmetric port,

degrading the separation between the sensing of the l_+ and l_s degrees of freedom. The fraction of f_1 sideband power exiting the asymmetric port of the BS is small but non-zero (about 10%).

5.3.6 Signal recycling cavity

Finally, we must determine the length of the signal recycling cavity (SRC). If we put the signal recycling mirror in the same chamber as the BS and PRM, then we want the SRC to be roughly the same length as the PRC. If we put the SRM in the output optic chamber, then L_{SRC} must be between 0.8 and 1.5 meters longer than L_{PRC} . We want the f_2 sidebands to be resonant in the SRC.

However, the carrier light will be detuned in the SRC; not resonant. The carrier detune in the SRC is chosen to give a peak in the transfer function at some frequency $f_{pk} = \omega_{pk}/2\pi$. The detune frequency is given by [24]:

$$d\nu_s = \frac{1}{\pi} \left\{ \tan^{-1} \left[\frac{(1 - L_{ITM} - R_{ITM}) \sin(\omega_{pk}\tau_{arm})}{r_{ITM}/r_{ETM}(1 + (1 - L_{ITM})R_{ETM}) - (1 - L_{ITM} + R_{ITM}) \cos(\omega_{pk}\tau_{arm})} \right] - \frac{L_{SRC}}{L_{arm}} \omega_{pk}\tau_{arm} \right\},$$

where the L 's are power losses, R 's are power reflectivities, and r 's are amplitude reflectivities. The arm cavity round-trip travel time is $\tau_{arm} = 2L_{arm}/c$.

We choose a peak frequency well above the arm cavity pole of 1591 Hz, at 4000 Hz. This gives a carrier detune in the SRC of $d\nu_s = 0.235$, or a one-way carrier phase shift of $d\phi_s = 0.235\pi/2$ radians.

We can then make the f_2 sidebands resonant in the SRC, if $L_{SRC} = (n_5 + d\nu_s)(c/2f_2) - L_{PRC}$ where n_5 is an integer. Choosing $n_5 = 5$ gives $L_{SRC} = 2.151$ m, or 10 cm shorter than L_{PRC} . This can be accommodated in the BS chamber.

5.3.7 Summary of lengths and frequencies

All these cavity lengths are *optical* path lengths; physical distances will be a bit smaller due to light travelling through glass.

Parasitic frequencies exist at $\pm f_2 \pm f_1 = \pm 132.8$ MHz and ± 199.2 MHz. THE LSC AIC group believe that these are not a problem; their effect on the signal extraction is under study.

Table 1 summarizes all the frequencies and lengths. They satisfy the following resonant conditions:

$$\begin{aligned} L_{MC} &= n_1 \frac{c}{2f_1}, & n_1 &= 3; \\ L_{PRC} &= (n_2 + 1/2) \frac{c}{2f_1}, & n_2 &= 0; \\ L_{ARM} &= (n_3 + 1/2) \frac{c}{2f_1}, & n_3 &= 8.05. \\ f_2 &= n_4 f_1, & n_4 &= 5; \\ L_{SRC} &= (n_5 - d\nu_s/2) \frac{c}{2f_2} - L_{PRC}, & n_5 &= 5, \quad d\nu = 0.235 \end{aligned}$$

Table 1: Parameters for several LIGO interferometers: the 40m in 1998 (recycling experiment), the Initial LIGO 4K interferometers, the 40m in 2002 (dual recycling for Advanced LIGO), and Advanced LIGO 4K. All lengths are *optical* path lengths. Physical path lengths are shorter due to extra path through optics. The Advanced LIGO numbers are not at all official; they're just our strawman design to complement the 40m design. All these optical parameters need to be carefully reviewed!

Parameter	40m (1998)	LIGO 4K	40m(2002)	Adv LIGO	units
Carrier λ	514.5	1064.	1064.	1064.	nm
Transmissivity T(ETM)	1.2E-5	1.5E-5	1.0E-5	1.0E-5	
Transmissivity T(ITM)	0.00565	0.02995	0.005	0.005	
Transmissivity T(RM)	0.1375	0.0244	0.07	0.07	
Mode cleaner length	1.0	12.255	13.542	16.655	m
FSR _{MC}	150.	12.23	11.07	9.00	MHz
RF freq1 $f_1 = n_1 f_{sr_{mc}}$	32.7	24.46	33.207	9.00	MHz
Arm Cavity L_{arm}	38.25	3999.	38.55	3999.	m
PR Cavity L_{PRC}	2.294	9.191	2.257	8.328	m
PRM-BS length	0.25	4.396	0.30	4.000	m
BS-ITMinline length	2.315	4.877	2.183	4.536	m
BS-ITMperpin length	1.773	4.599	1.731	4.119	m
Schnupp Asymmetry length	0.542	0.278	0.451	0.416	m
Arm cavity pole freq	1814	91	1578	15	Hz
Arm Cavity Finesse	1080	205	1235	1235	
Rec Cavity Finesse	24	138	47	47	
Arm Cavity power gain	670	130	775	775	
Rec Cavity power gain	9	48	16.5	16.5	
mirror diameter	10.16	25.0	12.5	31.4	cm
mirror length	8.89	10.0	5.0	13.0	cm
mirror mass	1.58	10.8	1.35	40.0	kg
PRM ROC	flat	8700	348	8700	m
ITM ROC	flat	14540	flat	14540	m
ETM ROC	61	7400	57.375	7400	m
n_1	-	3	3	1	
n_2	0	1	0	0	
n_3	7.84	652.13	8.05	239.61	
n_4			0	0	
n_5			5	21	
RF freq2 $f_2 = n_4 f_1$			166.033	180.0	MHz
SR Cavity L_{SRC}			2.151	9.148	m
SRM-BS length			0.200	3.821	m
RSE peak frequency			4000	300	Hz
Signal Cavity tune			0.235	0.038	rad/ $(\pi/2)$
SRM ROC			365	9000	m

5.3.8 DC detection

Finally, in order to implement DC detection of the GW signal, we need to let a little bit of carrier light out the dark port. This can be done either by slightly offsetting the arms from exact resonance (in opposite directions in the two arms), or by offsetting the Michelson asymmetry. The former is better, since the light so leaked has been filtered by the arms and thus is far less noisy. Arm offsets at the level of $\pm 5 \times 10^{-12}$ m, a small fraction of the cavity linewidth, will let a bit of carrier light out the dark port (1.3 mW for an input power of 1 watt). This has little effect on the fields anywhere else. No other changes are required to the optical configuration or controls. There is only small effect on the length control matrix.

The light exiting the dark port then consists of arm-filtered carrier light, possibly GW sidebands, as well as lots of RF sideband light (mostly f_2) and “junk” light in higher order modes (HOM) due to misalignments, imperfect Michelson contrast, *etc.*.

This light can be used to control several length and angular degrees of freedom, including the arm differential mode (L_- , the GW signal) and the Michelson length (l_-), by beating the carrier against the RF sidebands or the sidebands against each other.

The current plan for Advanced LIGO is to read out the GW signal via another path, in which the carrier is beat against the (audio) GW sidebands (homodyne or DC detection). A small, monolithic output mode cleaner (OMC) with cavity pole well below f_1 filters out all the HOM (non-TEM₀₀) and RF sideband light, thus dramatically reducing the shot noise at the photodiode. Only the filtered carrier light and GW sidebands make it through, and the (audio) beats between them on a DC photodiode are proportional to the GW sideband amplitude, and thus to h .

For example, the output mode cleaner can look just like the pre mode cleaner (PMC) of the existing Initial LIGO PSL [25]. The device is a fused silica spacer (approximately 8” by 2” by 2”) on which are glued three PZT-actuated mirrors forming a ring cavity. The reflectivity of the mirrors is chosen to achieve a pole frequency of 2 MHz.

6 Modeling

To obtain confidence in the design of the optical configuration and control scheme, we make use of a variety of simulations and models. These include:

- Twiddle [26] is used to verify the optical parameters, cavity lengths, RF sideband frequencies and resonance conditions described above for carrier and all sidebands, determine the DC fields at all points, predict the DC response at the photodetectors to all length changes (and thus the LSC control matrix), and predict the shape of the GW response function. Advanced LIGO and 40m configurations were developed simultaneously, following parallel paths.
- ModalModel [27] is a Mathematica program that is used to propagate mirror misalignments through to output ports, in order to design a wavefront sensing alignment sensing and control matrix.
- E2E [28] is used to further verify everything that Twiddle predicts, but in the presence of semi-realistic noise and dynamics. In particular, the degradation of the LSC control matrix in the presence of noise can be studied. Then, the model can be used to simulate lock acquisition dynamics, for development of lock acquisition software (as has been pursued by Matt Evans for Initial LIGO [29]).

- FFT [30] is used to study the degradation of the DC response of the IFO in the presence of optical imperfections and misalignments, in order to establish tolerance specifications for optics polishing and coating, and alignment control.
- Mechanics and local damping control of suspensions for 5" test masses are modeled using Simulink [31].
- Various Matlab models are used to predict fundamental noise sources (BENCH [22] and `noise_40m.m` [32]), propagate laser noise (`rnoise.m` [32, 33]), calculate mirror radii of curvature and gaussian beam optics (`propagate.m`), predict properties of the 12m mode cleaner (`mc_trans.m`), predict properties of the seismic stacks (`stacks.m`, `trstacis.m`), *etc.*
- Thermal lensing effects can be modeled using `Melody` [34]. Since such effects are estimated to be negligible (see section 8), this effort is not high priority (although it would be interesting to pursue).

These are discussed in the following sections.

6.1 Twiddle Model

A Twiddle [26] model has been used to verify the resonance conditions described above (Table 2), determine the DC fields at all points (Table 3), predict the DC response at the photodetectors to all length changes (and thus the LSC control matrix) (Table 4), and predict the shape of the GW response function (Fig 4). Preliminary work was reported in [35], which is superseded by the work presented here.

Because of the signal cavity detuning, the sideband fields everywhere in the IFO are asymmetric (different power for $+f_1$ sideband than for $-f_1$, and similarly for $\pm f_2$). Only one sideband in a pair is useful for length sensing. The consequent loss in length sensing sensitivity is compensated for by the increased sensitivity in the shot noise dip region. And, it has no effect on the GW DC readout sensitivity.

In these tables and figures, there is no arm DC offset, so no carrier light leaks out the dark port for DC detection. The addition of a small, balanced arm DC offset makes little change to anything except the amount of carrier light exiting the dark port.

These numbers are NOT final! Several things have not yet been optimized:

- There's sideband light in the arms, because the sidebands are not near antiresonance. We need to find out how much we can push the ratio L_{ARM}/L_{MC} towards the nearest resonant condition, given the vacuum envelope. This will improve the LSC matrix diagonality.
- Nominally, we have specified the pickoff reflectivities to be the same as in Initial LIGO: the AR-coating of the two ITMs and the BS have a reflectivity of 600 ppm.
- We need to optimize the modulation depths, the pickoff reflectivity, and (what else? XXX).
- We may want to optimize T_{SRM} , and even T_{PRM} (but remember, we are not trying to optimize our response to binary inspirals; we're trying to maximize our fidelity to Advanced LIGO).
- We can change the tune of the SRC, and thus the position of the peak in sensitivity. However, this would require a change in the macroscopic position of the SRM, so that the optical layout drawings would all have to be redone (which is not trivial because this is an extremely

Table 2: Various quantities characterizing the DC response of the 40m optics, (no arm offset).

T(ITM)	0.005
T(RM)	0.070
T(SM)	0.070
SRC carrier roundtrip tune	0.235π
Arm cavity pole frequency (Hz)	1578
Arm cavity carrier finesse	1235
PRC carrier finesse	47
Arm cavity carrier power gain	775
PRC carrier power gain	16.5
Sym Port carrier power reflectivity	0.006

Table 3: DC power in the 40m cavities (no arm offset) per one watt of input power. The signal cavity detuning produces an asymmetric response for the sideband pairs, thus, effectively, only one sideband is used for generating error signals.

frequency	$-f_2$	$-f_1$	carrier	f_1	f_2
Modulation depth Γ	0.1	0.1		0.1	0.1
Input from Laser	0.00249	0.00249	0.99003	0.00249	0.00249
Reflected (SP)	0.00249	0.00210	0.00620	0.00205	0.00003
Asym port (AP)	0.00000	0.00020	0.00000	0.00021	0.00233
PR Cavity	0.00010	0.08929	16.3827	0.10566	0.03334
SR Cavity	0.00010	0.00264	0.00000	0.00279	0.03095
Arm Cavity	0.00000	0.00005	6338.8	0.00007	0.00004

congested bit of real-estate, with three suspended optics within 30 cm of each other). In principle, the ROC of the SRM would have to change; but any small change would be well within tolerances.

- We must remember that the AdvLIGO optical configuration and control scheme is still not finalized, and is subject to change.

Things to note in Table 3:

- Input is 1 watt of laser power. modulation depth not optimized.
- All the carrier power everywhere agrees with naive analytic formulas.
- All carrier and sideband powers agree with E2E model! See below.
- No DC offset. When added, everything changes a little; and, of course, a little carrier light goes out the AP.
- Note the asymmetry between $-f_1$ and $+f_1$, and same for f_2 . This is an imbalanced IFO.
- Note significant $+f_2$ in SR and PR cavity. Little f_1 in SRC. This allows one to distinguish ΔL_{PRC} signals from ΔL_{SRC} .

Table 4: Length sensing signals. \otimes means double demodulation.

Signal	L_+	L_-	l_+	l_-	l_s
SP, f_1	15.2	0.000	-0.062	0.064	-0.001
AP, f_2	0	1.69	0	0.002	0
SP, $f_2 - f_1$	-0.0003	0.0001	0.214	0.029	0.039
AP, $f_2 \otimes f_1$	0	0	0.0025	-0.0034	-0.0004
PO, $f_2 - f_1$	0.005	-0.004	1.000	-0.277	-2.980

Table 5: Length sensing signals for Advanced LIGO. \otimes means double demodulation. These numbers agree, up to an overall constant, with the table Peter Fritchel showed at the August 2000 LSC meeting (LIGO-G000225).

Signal	L_+	L_-	l_+	l_-	l_s
SP, f_1	1890	0.00	-1.94	0.11	0.00
AP, f_2	0	-1500	0	-1.88	0
SP, $f_2 - f_1$	-0.11	-0.01	19.5	-0.11	8.66
AP, $f_2 \otimes f_1$	0.000	0.001	-0.031	0.242	0.005
PO, $f_2 - f_1$	-0.42	-0.01	8.84	5.81	245

- Only $+f_2$ used for control of arm cavities.
- Little (but non-zero) RF sideband light in arms.

Things to note in Table 5 and Fig. 4:

- Nomenclature is in flux for Advanced LIGO. L_+ is also known as Arm Common Mode; L_- is also known as Arm Differential Mode; l_+ is also known as power recycling cavity length L_{PRC} ; l_- is also known as differential Michelson length ΔL_M ; l_s is also known as signal recycling cavity length L_{SRC} or signal extraction cavity length L_{SEC} .
- The LSC control matrix, now 5×5 instead of 4×4 , is much more diagonal than in Initial LIGO, due to the presence of two pairs of RF sidebands to work with.
- Nonetheless, there is no signal in which the l_- (differential Michelson) degree of freedom dominates.
- The l_+ and l_- signals are not very robust, but neither are they at Initial LIGO.
- These numbers vary as one varies arm length, unmatched arms, imperfections, losses, *etc.*
- The pickoff (PO) signal must be multiplied by the PO power reflectance (600 ppm nominal). Is the signal big enough to be significantly above PD noise? Can make it bigger, with some sacrifice in PRC gain and thus GW shot noise response; maybe that's appropriate here. Ditto, for modulation depth.
- Double demodulation is difficult; it is hard to determine the demodulation phases experimentally.

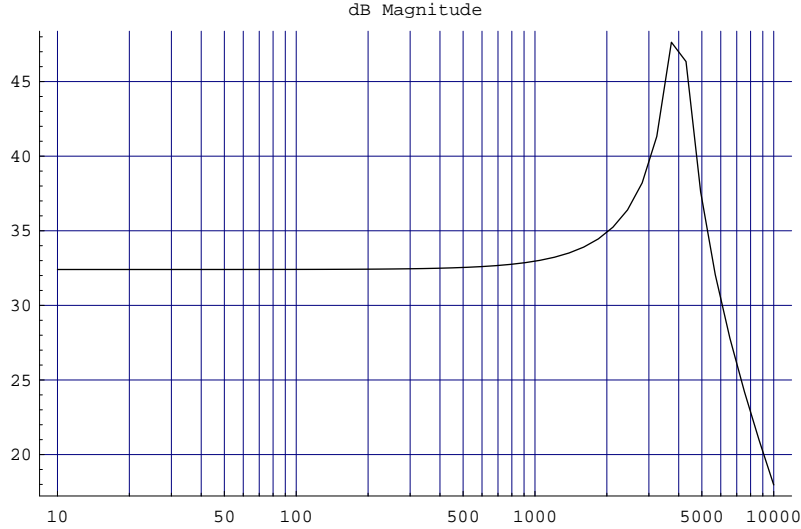


Figure 4: GW (L_-) response for 40m parameters, as predicted by Twiddle. The choice of signal cavity roundtrip detune of 0.5π produces a peak in the response, and a dip in the shot noise sensitivity, at around 1500 Hz.

- In Fig. 4, we see that several error signals have more than one zero-crossing of the control signal; that DOF can achieve lock at the wrong point. IFO experience tells us that even when this is so, the IFO can eventually achieve lock in the right place. locking at the wrong point in one DOF is often unstable when other DOF's acquire lock.
- Offset-locking the arms differentially lets some arm-filtered carrier light out the dark port. This has no effect on the sensitivity of the auxiliary length degrees of freedom, since they demodulate at $f_1 \pm f_2$, ie, they don't use the carrier. The effect on the L_+ sensing is small and inconsequential. The effect on L_- is to improve the sensitivity by a factor 2.
- It's time for a full lock acquisition study, with E2E. This takes some time. Meanwhile, there's some confidence that this is a workable scheme.
- Thanks to Jim Mason for all his help!

6.2 ModalModel Modeling

ModalModel [27] is a Mathematica program that is used to propagate mirror misalignments through to output ports, in order to design a wavefront sensing alignment control matrix.

See [36] for a preliminary study of the wavefront sensing at Advanced LIGO and the 40m, including the use of ModalModel to generate a alignment wavefront sensing and control matrix.

One conclusion from that study is that the presence of two pairs of RF sidebands make it unnecessary to have an additional reflected sideband, as is used for Initial LIGO.

That study made use of a control scheme that was somewhat different from the scheme that emerged in August, 2000. Updating those results using the currently envisioned control scheme is a high priority item.

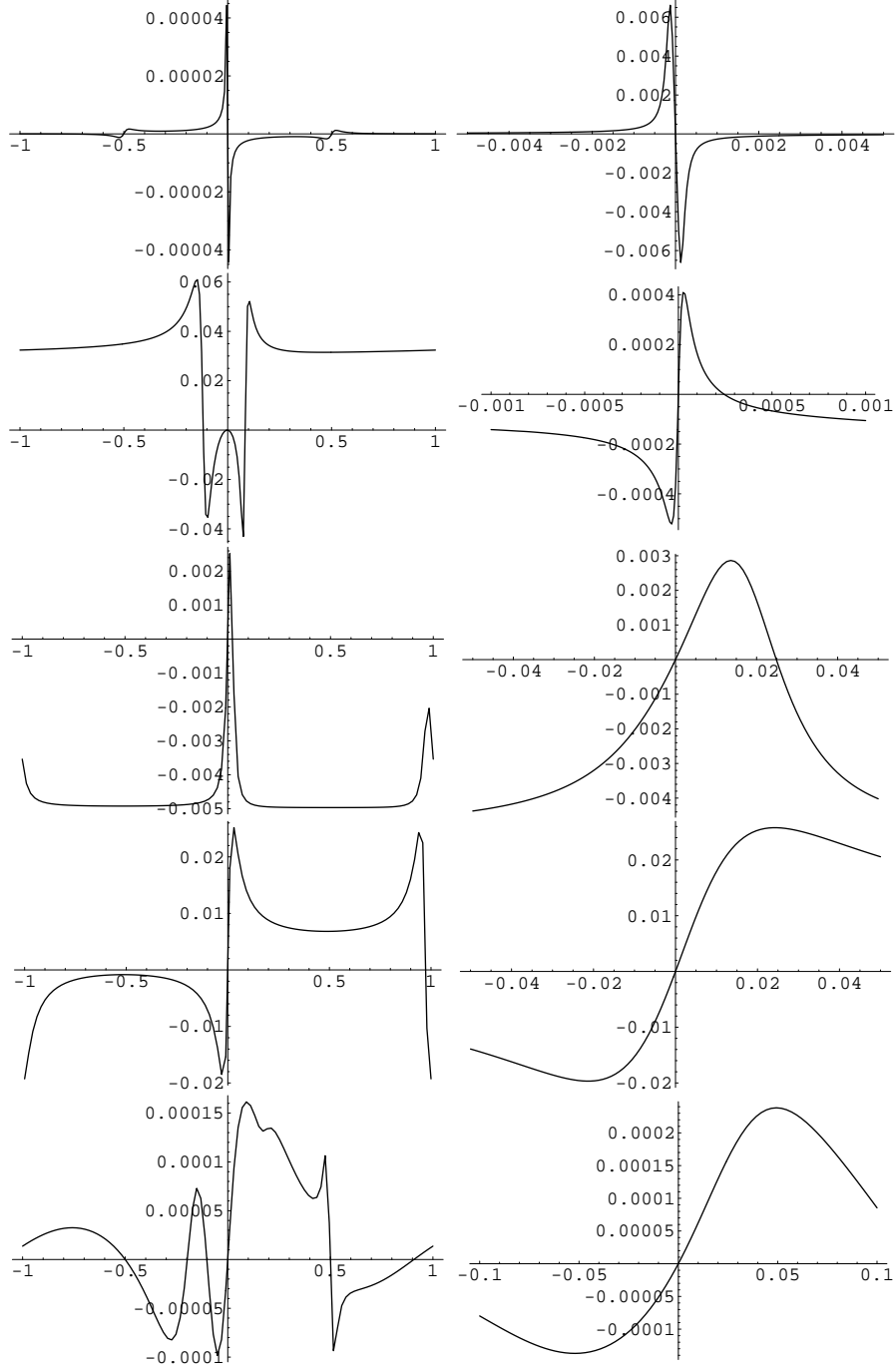


Figure 5: Predictions from Twiddle for error signal for each degree of freedom. Top row: Arm differential mode, at asym port, f_2 . 2nd row: Arm common mode, at symm port, f_1 . 3rd row: PRC length, at symm port, $f_2 - f_1$. 4th row: SRC length, at PO port, $f_2 - f_1$. 5th row: Michelson l_- , at asym port, $f_2 \otimes f_1$. In each case, the fig on the right is a zoom-in of the figure on the left, and the x-axis is the mirror motion in units of $\lambda/2\pi$.

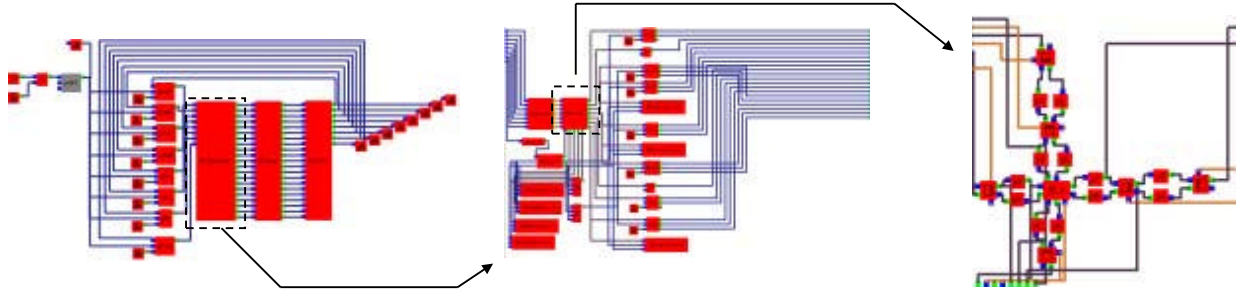


Figure 6: Some of the E2E “boxes” used to model the 40m dual-recycled interferometer.

6.3 End-To-End Modeling

E2E [28] is used to further verify everything that Twiddle predicts, but in the presence of semi-realistic noise and dynamics. In particular, the degradation of the LSC control matrix in the presence of noise can be studied. Then, the model can be used to simulate lock acquisition, for development of lock acquisition software (as has been pursued by Matt Evans for Initial LIGO [29]).

We modified the Han2K package of E2E “boxes” to produce a dual-recycled interferometer, with 7 core optics (see Fig. 6). E2E does not yet have a dual-recycled summation cavity, so we simply used primitive propagators, and added the signal mirror. Developing a dual-recycled summation cavity is an important task for the future.

E2E runs with a time-step that is roughly the one-way light travel time through the shortest propagator that has `HAVE_DELAY = true`. In our case, that is the distance between the signal recycling mirror and the summation cavity (around 0.2 m). On the other hand, in order for fields to build up to full strength in the arm cavities, the simulation must be run for a time corresponding to the round-trip light travel time through the arms, times the finesse, times another factor of 100–1000 (why this factor needs to be so large is not understood). Thus, even for perfect alignment and mirror positions, and in the absence of noise, one needs to run the simulation for $10^6 - 10^8$ time steps to build the fields up to their full strength. To get around this practical problem, for now, we have been running with `HAVE_DELAY = false` for all the short propagators. This allows us to study the DC fields everywhere in the interferometer, as well as the response of output port signals to slow mirror sweeps. Of course, the dynamics of lock acquisition will not be realistically reproduced if delays are turned off in the propagators.

We have verified that the DC fields everywhere in the interferometer, as predicted by E2E in the absence of noise, agree with the predictions from Twiddle and from analytical formulas, to excellent precision. This has been tested (a) for the untuned broadband RSE configuration; (b) for the tuned configuration; (c) with offset-locked arms for DC demodulation of the GW signal.

All this is in the absence of noise and global LSC control. The plan for the near term is:

- Turn on the seismic noise, and watch the IFO slowly fall out of lock.
- Then sweep mirrors, measure 5×5 linear control matrix, compare with Twiddle.
- Then implement a global LSC control loop (as a simple 5×5 linear control matrix), turn the noise back on, and watch the IFO *stay* in lock.
- Only THEN can we explore lock acquisition with a suitably generalized version of Matt’s guided lock code.

This last step is a difficult, long-term project.

6.4 FFT Modeling

FFT [30] is a FORTRAN program used to study the degradation of the DC response of the IFO in the presence of optical imperfections and misalignments, in order to establish tolerance specifications for optics polishing and coating, and alignment control.

Despite its misleading name, it is *not* a program to take FFT's; rather, it *uses* the NAL FFT program (and has recently been converted to use FFTW) to take 2-D Fourier transforms of the transverse profile of the beam everywhere in the interferometer in order to propagate the beams from optical element to optical element. The optical elements are modeled as 2-D spatial maps, which can represent imperfect or misaligned optics. Imperfections can be low-spatial-frequency distortions (astigmatisms, Zernicke distortions, tilts, *etc.*) mid-spatial-frequency surface roughness, or transmission imperfections. High-spatial-frequency micro-roughness, which generates low-angle scatters, are not simulated.

With these “realistic” maps, the fields are relaxed to a stable DC value. The amount of non-TEM₀₀ component to the beam is calculated, as well as the contrast defect and the level of “junk” light at the asymmetric port photodiode. This allows one to determine the DC strain sensitivity of the instrument. Turning it around, one can require limited degradation of the DC strain sensitivity, and thus obtain specifications for the level of tolerable misalignment, optical surface figure, and surface roughness (measured in fractions of a wavelength, *e.g.*, $\lambda/1200$).

Quantities which can be calculated with FFT in the presence of imperfect or misaligned optics include.

- FFT-optimized recycling mirror Reflectivity;
- FFT-optimized Schnupp asymmetry;
- FFT-optimized modulation depth;
- FFT-optimized mirror curvatures (due to Schnupp asymmetry);
- FFT-predicted arm gain and PRC gain;
- FFT-predicted carrier and SB power at APD;
- FFT-predicted contrast defect;
- FFT-predicted $h_{shot}(0)$.

Table 6 represents the beginnings of a table which can be fleshed out in order to establish specifications for optical quality of Advanced LIGO and the 40m.

This work is being pursued, for the 40m and for Advanced LIGO, by the CSUDH group [37] (as specified in their MOU to the LIGO Lab).

Table 6: The beginnings of a table which can be fleshed out in order to establish specifications for optical quality of Advanced LIGO and the 40m.

RMS deformation	0	$\lambda/1800$	$\lambda/1200$	$\lambda/ 800$	$\lambda/ 400$
RMS deformation (nm)	0	0.59	0.89	1.33	2.66
R_{RM} (%)	68.4				
Opt. Asymm (cm)	45.5				
Mod Depth Gamma	0.36				
G_{prec} , Carr, TEM00	8.9				
G_{arm} , Carr, TEM00	2600				
G_{APD} , Carr, TEM00	5e-3				
G_{APD} , Carr, Total	6e-3				
1-C	1.6e-3				
G_{prec} , SB, TEM00	7.2				
G_{APD} , SB, TEM00	0.95				
G_{APD} , SB, Total	0.95				
R_{ref} , Total	0.015				
f_{pole} (Hz)	2022				
$h_{SN}(0)$ (1e-22)	1.8				

7 Suspended optical components

The 40m prototype upgrade will (initially) contain three suspended optics for the 12m mode cleaner, and 7 core optics (PRM, SRM, BS, two ITMs, and two ETMs).

We may need to develop a suspended monolithic output mode cleaner. Other in-vacuum optics, including the mode matching telescope and steering mirrors (which are suspended in LIGO I) will be fixed on the optical tables at the 40m. This is primarily due to lack of in-vacuum real estate for suspensions. We can get away with it because there is low priority for “heroic” efforts to reduce noise from these sources in the GW signal.

With the optical configuration to be described below, the beam is everywhere (from the 12m mode cleaner on) on the order of $w_0 \sim \sqrt{\lambda L_{arm}/\pi} \sim 4.0$ mm in transverse dimension (amplitude $1/e$ radius). Since the arms will be half-symmetric with flat ITMs, it’s actually $w_0 \sim 3.1$ mm. This corresponds to a power $1/e$ diameter of $r_0 = \sqrt{2}w_0 \sim 4.4$ mm, and power 1ppm diameter of $d_{1ppm} \approx 5.25w_0 \sim 16$ mm.

Because of the inevitable misalignments, and to play it safe, we require 30 mm clear aperture for all optics except for the beam splitter, where we require a factor $1/\sin(45^\circ) = 1.4$ larger clear aperture (in the horizontal direction).

OSEM sensor/actuators have an outer diameter of 25 mm and are centered 3 mm radially from the edge of the optic. Consequently to ensure a 50 mm clear aperture, the optic must be at least 75 mm in diameter (3”). The beam splitter (and MC flat mirrors) are at 45° to the beam, but the OSEMs for these optics can be placed further to the top and bottom of the optic, ensuring maximal clear aperture in the horizontal dimension. This is probably sufficient for all optics except for the test masses (ITMs and ETMs), as discussed below.

LIGO I input suspended optics [38] (mode cleaner and mode matching telescope) use 3” diameter, 1” thick (more precisely, 75mm diameter, 25mm thick), on SOS suspensions [39]. These optics and suspensions are fully engineered and relatively well understood; some 20 of them have been built for LIGO I. They appear to be entirely appropriate for use in the 40m prototype upgrade, for the 12m mode cleaner and for the PRM, SRM, and BS.

7.1 Choice of test mass optic size and aspect ratio

The four test mass optics (ITMs and ETMs) contribute thermal noise to the GW signal. As discussed below, this test mass thermal noise will likely dominate the entire GW noise spectrum above 100 Hz; therefore, some effort should be made to minimize it.

Thermal noise in the GW channel is generically of the form

$$S_x^{thermal} \sim \left(\frac{\tilde{h}L}{2} \right)^2 = \frac{4k_B T}{m\omega} \sum_n \left[\frac{\alpha_n \omega_n^2 \phi_n(\omega)}{(\omega_n^2 - \omega^2)^2 + \omega_n^2 \phi_n^2} \right]$$

where S_x is the displacement noise power spectrum, \tilde{h} is the equivalent GW noise power spectrum, k_B is Boltzmann’s constant, T is the temperature, $\omega = 2\pi f$ is the GW frequency, m is the mass of the test mass, and the sum is over normal modes of vibration with resonant frequency $\omega_n = 2\pi f_n$, effective mass [41] α_n , and loss angle ϕ_n .

There are two sources of thermal noise that are relevant here: suspension thermal noise (pendulum and wire violin modes), and internal test mass thermal vibrations.

Suspension thermal noise in \tilde{h} scales like $1/\sqrt{m}$, so larger masses reduce this. The pendulum thermal noise peaks at the pendulum frequency of $f_0 = 1$ Hz and falls like $1/f^{3/2}$. Above 100 Hz,

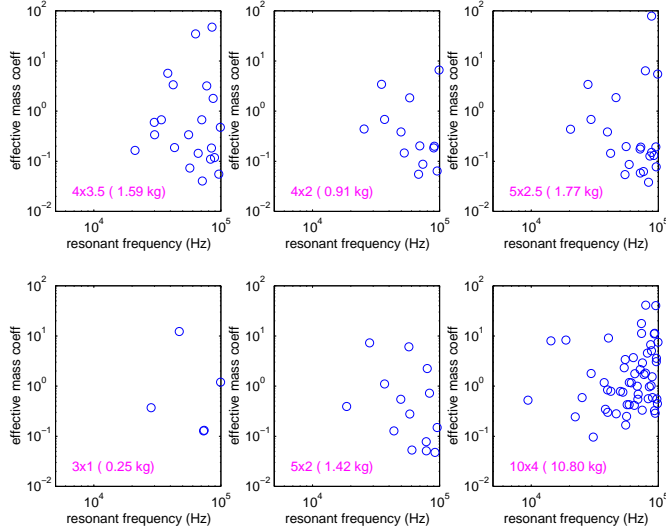


Figure 7: Frequencies and effective masses of the node 0 (drumhead and breathing) modes of a right-circular cylinder of the dimensions shown [41].

it is negligible at the 40m (see noise discussion below). The wire violin modes have resonances that are right in the detection band, and they have very high $Q = 1/\phi_n(\omega_n)$. Although they may have some impact on a GW signal search, they are not a problem for the 40m program. The noise lines at discrete frequencies in the GW channel may even serve as a useful sign-post in diagnosing the IFO. Nonetheless, they can be minimized by choosing a large mass.

The test masses have natural resonant frequencies which, for the optic sizes we are considering (much smaller than LIGO), are well beyond the Nyquist frequency of our 16kHz ADCs. The frequencies and effective masses of the node 0 (drumhead and breathing) modes, calculated with `testmass5.c` [41], are shown in Fig. 7.

These internal resonances have high Q and thus leak only a little into the GW frequency band via dissipation, at a level $\tilde{h} \sim \phi_n$. We thus want to minimize the loss ϕ_n . How does this scale with test mass size and aspect ratio?

The intrinsic loss of fused silica should depend only on the anelastic property of the material, and thus is not expected to scale with mass. This loss is very small, on the order of 10^{-7} ; this is a primary reason why fused silica is the material of choice for LIGO I (and why sapphire may be even better for Advanced LIGO).

Our test masses will have attachments (standoffs) for the suspension wires and the actuator magnets. These provide a loss mechanism which dominates the total loss in our test masses. The loss is given by

$$\phi(f) \sim \frac{dU/dt}{2\pi fU}$$

where U is the total energy stored in the optic. The attachments present a “hole” for energy leakage, proportional to the area A of the attachment on the test mass surface and to a “coupling” κ which depends on the “softness” of the attachment, the position of the attachment relative to the spatially varying vibrational mode, *etc.*. With an energy density u and volume V , $U = uV$, and $dU/dt \sim \kappa uA$, so that $\phi(f) \sim \kappa A/V$. Assuming the attachment area is fixed, independent of test mass size, this suggests that larger masses have less loss due to attachments; as this loss dominates,

we can minimize thermal noise by maximizing the test mass size.

For intrinsic loss, it is assumed that κ grows linearly with f , so that $\phi(f) = 1/Q(f)$ is independent of frequency. For attachment loss, we might assume κ is roughly independent of frequency.

What about aspect ratio (optic radius to thickness)? The thinner the optic, the less beam loss due to absorption and scatter. But it also leads to lower-frequency vibrational modes (saddle and drum-head), which may come close to the GW signal and IFO control frequency bands. This was of some concern for the rather thin LIGO beam splitter [42], and it presumably played a role in determining the optimal aspect ratio for the LIGO core optics [43]. This is not a concern for the small optics used at the 40m.

In [44], it is shown that the internal thermal noise is a weak function of aspect ratio, with thicker optics preferred. It's a very weak function, however; and internal thermal noise does not dominate for us.

Stan Whitcomb [45] has suggested that the LIGO aspect ratio (10" diameter, 4" thick) "may reduce undesirable parasitic torques from sideways forces on the magnets".

There are also practical matters to consider, such as price and availability of the optic blanks, polishing, hanging and balancing. However, these don't seem to be significant in driving a decision [46].

We can have relatively large mass and "understood" (ie, LIGO I) aspect ratio, by choosing test masses with 5" diameter, 2" thickness. This gives 1.4 kg test masses. They can be purchased, polished, and coated with acceptable cost and schedule, and can be hung on a straightforwardly-scaled up LIGO SOS suspension [46]. This is what we choose, for the two ITMs and two ETMs.

7.2 Specifications for suspended optics

Specifications must be established for the the suspended optics mirror blank material, polishing, and coating.

Specification details and drawings are in the 40m COC web page [49]. Here we summarize. Mirror blank material specifications:

- Dimensions for the two MC flat mirrors, the MC curved mirror, the PRM, SRM, and BS: 78_{-0}^{+1} mm diameter, 28_{-0}^{+1} mm thickness.
- Dimensions for the four test masses: 125_{-0}^{+1} mm diameter, 50_{-0}^{+1} mm thickness.
- Clear aperture: central 30 mm for all optics except for the BS and the two MC flat mirrors, which are 70 mm horizontal.
- Material: fused silica. For the BS and ITMs, through which significant power passes, we choose low-absorption Heraeus SV glass (< 1 ppm/cm absorption). For all the other optics, we can live with < 20 ppm/cm absorption, as achievable with Corning glass.
- Limits on defects, homogeneity, absorption, birefringence, bubbles and inclusions.

Mirror polishing specifications:

- Sides and bevels polished to transparency.
- Limits on number and size of scratches and point defects.

- Surfaces are nominally flat or spherical concave. Concave surfaces have specified radius of curvature (see below) with tolerances, and a limit on astigmatism (typically: ≤ 10 nm).
- Surface errors are specified as a limit on rms deviation from the best fit spherical surface, as measured from phase maps.
 - Low spatial frequency (≤ 4.3 cm⁻¹) contributing to small angle scattering: typically $\sigma \leq 0.8$ nm.
 - High spatial frequency (4.3–7, 500 cm⁻¹) contributing to large angle scattering: typically $\sigma \leq 0.1$ nm. This corresponds to “super-polish”.

These specs require detailed modeling to establish. These studies are in progress (Ganezer for FFT, and Mike Smith for scattering noise). While we wait, it is best to specify the best performance that can be achieved with established techniques, which are good enough for LIGO; hence, the “typical” numbers given above.

- Wedge angles. These have been specified by Mike Smith (see Tables 8 and 7) to provide adequate separation of secondary beams for pick-offs and baffling (all in the horizontal plane).

Mirror coating specs:

- Coatings are for $\lambda = 1064$ nm.
- Angle of incidence to be 0° for the PRM, SRM, ITMs, ETMs, and MCcurved; 45° for the BS and two flat MC mirrors.
- Surface 1 (high-reflectivity): specified power transmission (see below).
- Surface 2 (anti-reflection coating): reflection of (600 ± 100) ppm.
- limits on non-uniformity, scatter, and absorption.
- Mike Smith has determined that light scattering from the baffles back to the test masses can send significant amounts of scattered light back into the IFO. In order to limit this, we will only coat a portion of the high-reflectivity surface of the test mass mirrors; only scattered light incident on this central portion has a chance of getting back in. The beam sizes at the ITMs and ETMs are 3.03 and 5.24 mm, respectively; the 1ppm diameters are thus 15.9 and 27.5 mm, respectively. However, we should give ourselves some room for tolerance against misalignments (deliberate and unintentional); I guess that an additional 10mm provides some extra room. SO, the plan is to coat only the central 40 mm (diameter) of the test mass optics, rather than the full 125 mm diameter. Garilynn says that this is no problem.

7.3 Radii of curvature

We can make the cavity symmetric (ITM and ETM with equal curvature, beam waist half-way between), half-symmetric (ITM flat, ETM curved, beam waist at ITM), or somewhere in between (The LIGO I beam waist is a bit closer to the ETM, in order to keep the spot size at the ETM below some limit).

There are no compelling arguments for any choice, here. However, choosing a flat ITM means: (a) placing the waist at the ITM means that one can directly measure it with the ITM camera; (b)

the beam is a bit smaller in the input optics than it might otherwise be; (c) it might be faster to get a nominally flat replacement optic, if necessary.

We therefore choose half-symmetric arm cavities, with flat ITMs.

We choose an arm cavity g-factor (see Appendix) of $1/3$, for optimal stability. We can instead opt for larger g-factors and thus larger beams, thereby reducing the test mass thermal noise somewhat. Increasing g up to 0.95 increases the spot size at the ETM by $\sim 50\%$, decreasing the thermal noise by $\sim 21\%$. We prefer to work conservatively with a more stable cavity, as envisioned for Advanced LIGO; thus, we'll stick with $g = 1/3$ unless Advanced LIGO plans change.

The arm cavities will be of equal length; nominally, 38.25 m. Therefore, the ROC of the ETM shall be 57.375 m. It is reasonable to expect a few percent tolerance on this number from the polishing process. However, we must require that the two ETMs have the same ROC to 1% (see Appendix).

The beams from the arms propagate through the 50 mm thick ITM (with $n = 1.4496$), then through an *average* of 1.80 meters to the beam splitter. In the current design of the readout scheme, the PRM is 300 mm from the BS, and the SRM is 200 mm from the BS. This determines the beam spot sizes and ROC of all the core optics, as specified in Table 7. Note that thermal lensing effects are being neglected here; see section 8.

In each case, we determine tolerances on the ROC by requiring that the incoming beam be mode-matched to the arm cavity beam, with higher order mode loss of 1%.

The Schnupp asymmetry produces different-sized spots on the BS: Transmitted arm: $w = 3.108$ mm; Reflected arm: $w = 2.953$ mm; *AveragePRC* : $w = 3.033$ mm. This corresponds to deviations from the average of $\pm 2.5\%$. We require that the arm optics are sufficiently well matched that they produce a contrast defect at the beam splitter that is no larger than the inevitable contrast defect resulting from the Schnupp asymmetry.

In the end, tolerances on the radius of curvature are driven by what is do-able by the polishing vendors, and what is measureable. From previous LIGO experience, and from conversations with the vendors, it appears that it is possible to achieve a tolerance of 20 nm sag across the central 30 mm of the optic. This will allow us to meet the tolerance criteria discussed above. It produces the ROC tolerances listed in Table 7.

The cavity lengths are fixed by the analysis in section 5.3. These are optical path lengths. Since optical phase advances more slowly through glass, the physical path lengths are larger, by:

$$\delta_{ITM}(n-1)/n = 50(0.45/1.45) = 15.5\text{mm (ITMS)}$$

$$\delta_{BS}(n-1)/n = 2.8\sqrt{2}(0.45/1.45) = 12.3\text{mm (BS)}.$$

7.4 Mode Cleaner optics

For now, the mode cleaner configuration is planned to be a duplicate of the LIGO I 4K version [38].

The cavity length will be a bit longer (12.246m for LIGO 4K, 12.690m for the 40m). We keep the same g-factor of 0.29, so the ROC of the curved mirror (MC2) goes from 17.25m to 17.87 m, with roughly 2% tolerances. We keep the same mirror dimensions, materials, polishing, and transmittances. These are as summarized in Table 7.

7.5 Coatings

As discussed above, we endeavor to make the 40m optical configuration as close as possible to what is planned for Advanced LIGO (mirror transmissions, cavity finesse; *not* arm cavity storage time!).

The the core optics coatings are as specified for Advanced LIGO in refs [47] and [48].

- The power transmissivities for the ITM (0.5%) and the signal mirror (0.7%) are design parameters for Advanced LIGO, and will be used for the 40m.
- For Advanced LIGO, the SRM transmission maximizes the CBI reach. For the 40m, this gives a strong peak in the RSE response function, easy to see. The SRC is not so high in finesse as to be difficult to control.
- For Advanced LIGO, the ITM transmission maximizes the CBI reach. For the 40m, we want the same finesse in the arms as in AdvLIGO. The common-mode tolerance is estimated by requiring the reflectivity of the IFO to stay in the over-coupled region for a fixed PRM transmissivity of 7%. The differential tolerance is estimated by requiring the resulting contrast defect to be no bigger than 300ppm. A tighter tolerance of $(0.50 \pm 0.01)\%$ would be desirable!
- The power transmissivities for the ETMs are specified to be 15 ± 5 ppm as in Initial LIGO. For Advanced LIGO and the 40m, it is assumed that any ETM transmission is to be counted as part of the 37.5 ppm total ETM loss. For Advanced LIGO, the spec is > 1 ppm, because it operates at high power; the 40m needs to see the light even with 0.1 w of input light.
- For the PRM, we want a transmissivity that almost critically couples with the rest of the Michelson, but is slightly over-coupled, to let some light back to the symmetric port for IFO control. The reflectivity of the Michelson depends on all the losses, and cannot be predicted reliably in advance. Thus, we will have 3 optics with three different transmissivities: $(6.5 + -0.7)\%$, $(7.0 + -0.7)\%$, and $(8.0 + -0.7)\%$. Note that ref. [47] says “ $T(\text{PRM}) \sim 6\%$ ”, but my Twiddle simulations suggest that this would yield an under-coupled IFO; $T(\text{PRM})$ needs to be 6.5 for an over-coupled IFO ($r(\text{front}) < r(\text{back})$).

In addition, the anti-reflective (side 2) coatings are chosen as follows:

- We want pickoff beams from the BS and ITMs;
- and there’s no harm in also having a pickoff beam at the PRM just in case (although we also have an “initial pointing beam”). But we’ll get sufficient beam with a standard ≈ 300 ppm coating.
- In principle, we should optimize the pickoff amount (trading off PRC loss, which reduces PRC gain, for sufficient pickoff signal). However, this is not a critical issue for the 40m, so we can stick with the Initial-LIGO and AdvLIGO spec of 600 ppm.
- NOTE that this builds in 1200 ppm of loss, minimum, in the PRC cavity. For modelling, assume 1500-2000 ppm of loss, total.

So, we choose anti-reflective coating for side 2 with reflectivity of 600 ± 100 ppm for BS, ITM, and < 300 ppm for PRM, SRM, ETM, and all 3 mode cleaner mirrors.

The detailed coating specifications are in ref. [49] and are summarized in Table 7 and Fig. 8.

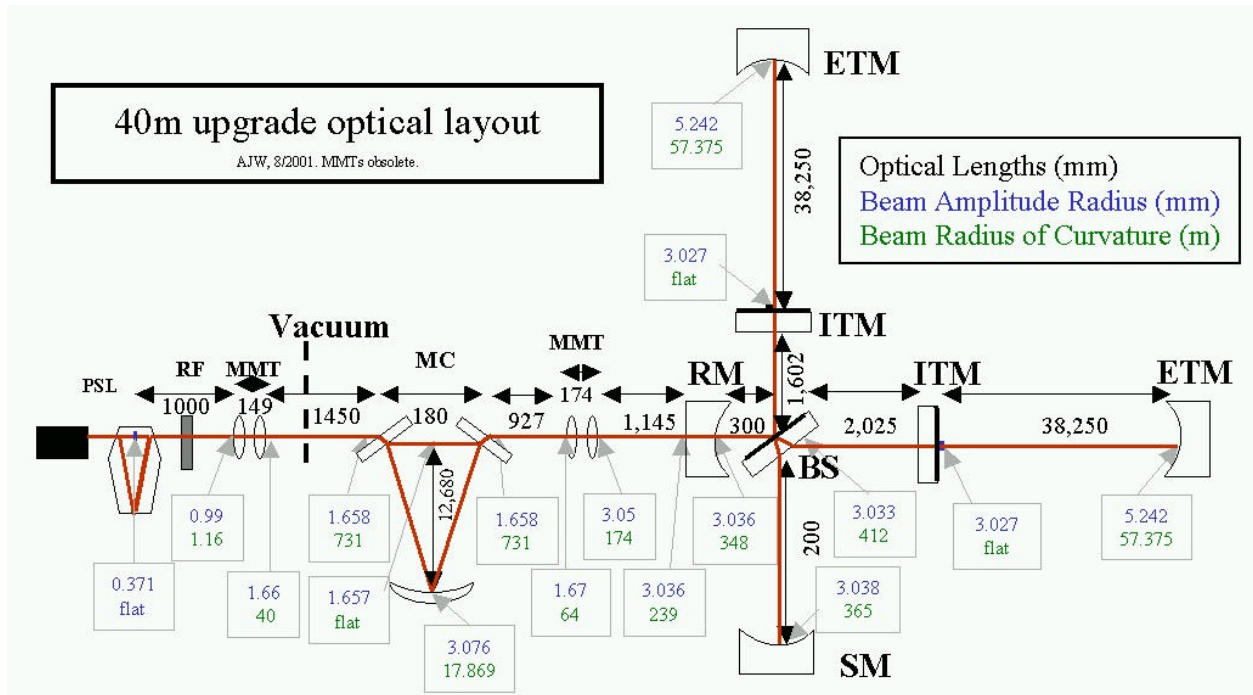


Figure 8: Cavity lengths, beam widths, and ROC at all optics for the 40m prototype upgrade.

8 Thermal lensing

The absorption of laser power on the suspended optics heats the fused silica, causing thermal expansion and a shift in the index of refraction (dn/dT), both of which can lead to a distorted laser beam and degradation of the mode matching in the interferometer.

Estimates of the thermal expansion and dn/dT of fused silica have also been made: thermal expansion $= \alpha = 0.51 \times 10^{-6}/^\circ K$, $dn/dT \equiv \beta = 8.7 \times 10^{-6}/^\circ K$. It can be seen that dn/dT is the dominant effect.

Both effects cause a change in the face of the optic. The sagitta s of the optic over an area defined by the width of the beam w is determined by the specified radius of curvature $ROC \approx w^2/(4s)$. A change δs in the desired sagitta produces a corresponding change in the radius of curvature,

Table 7: Suspended optic mirror parameters for the 40m prototype upgrade.

Mirror	diameter (mm)	thickness (mm)	mass (kg)	wedge (deg)	ROC (m)	ROctol (m)	spot w (mm)	power T	R(AR side)
PRM	75	25	0.225	2.5	348	± 23	3.04	$(7.0 \pm 0.7)\%$	< 300 ppm
SRM	75	25	0.225	2.5	365	± 25	3.04	$(7.0 \pm 0.7)\%$	< 300 ppm
BS	75	25	0.235	1.0	flat	> 5625	3.03	50.0%	(600 ± 100) ppm
ITMs	125	50	1.320	1.0	flat	> 5625	3.03	$(0.5 \pm 0.05)\%$	(600 ± 100) ppm
ETMs	125	50	1.276	2.5	57.37	± 0.6	5.24	15ppm	< 300 ppm
MC1, MC3	75	25	0.235	0.5	flat	> 5625	1.66	$0.2\% \pm 100$ ppm	< 300 ppm
MC2	75	25	0.225	0.5	17.87	± 0.35	3.08	10ppm	< 300 ppm

and thus in the position and size of the beam waist defined by the optical cavity containing the distorted optic.

The changes δs in the desired sagitta due to thermal expansion and dn/dT are given by [40]

$$\delta s = \frac{\alpha}{4\pi\kappa}P_a + \frac{\beta}{4\pi\kappa}P_a + 1.3\frac{\beta}{4\pi\kappa}p_a d,$$

where $\kappa = 1.38 \text{ W/m/}^\circ\text{K}$ is the thermal conductivity, P_a is the power absorbed on the coating, $p_a d$ is the power absorbed in the bulk (of thickness d).

Power is absorbed by the HR coatings on the optics, the AR coatings, and in the bulk. Estimates of the absorption in each of these elements have been made and incorporated into Melody [34].

Using an input power of 1 watt, a PRC power gain of 17, and an arm power gain of 775, we estimate that the ROC of the ITM changes from ∞ to 511 m, and the ROC of the ETM changes from 57.375 m to 51.9 m. This produces a power mode mismatch into the arms of 0.5. This is presumably tolerable.

9 Suspensions

In the first incarnation of the upgraded 40m ifo, we will focus on the control of the dual-recycled optical configuration. Learning how to control prototypes of advanced (multiple pendulum) suspensions at the same time will be difficult, so we choose to start with LIGO I-like single pendulum suspensions, which will have been well characterized and understood within the coming year.

Following this, we *may* choose to implement (scaled-down) prototypes of multiple pendula, if the overall goals of the Advanced LIGO R&D work calls for it. Full scale Advanced LIGO multiple pendulum suspensions cannot be accommodated in the 40m vacuum chambers; these will be tested at the LASTI facility at MIT.

9.1 Suspension mechanical

We will need two types of mechanical suspensions for the 40m upgrade, to support the two sizes of optics we will be using (75 mm dia. X 25 mm thick and 125mm dia. X 50mm). The 75x25 suspensions can be exact replicas of the SOS suspensions currently in use at LIGO for the mode cleaner and mode-matching telescope [39], with modifications to reflect lessons learned during LIGO I commissioning (improved sensor/actuators).

The 125x50 suspensions can be simply scaled-up versions of the existing SOS suspensions (work by Janeen Romie). Both suspension types will use the redesigned LIGO I sensor/actuator heads (“osems”).

The larger suspensions have been designed so that the various resonant frequencies are shifted somewhat from those of the LIGO SOS suspensions, to make it easier to diagnose problems.

The AR-coated optic face has a wedge angle in order to avoid etalon effects, to provide a pick-off beam, and to permit baffling of undesired reflections. The flat optics (BS, MCF1, MCF2) are wedged symmetrically. All wedges send the reflected beam off horizontally, either to the right or left. All suspensions and fixtures are designed for specific wedge angles and orientations.

The suspension cages are made of stainless steel and aluminum. The wire, suspension block, wire standoffs, magnets and standoffs, sensor/actuator heads and head holders, safety cage and safety stops, and cables and cable harnesses, would be as described in [39].

The 1ppm diameter of the beam spot in the vertex area is 16 mm. The open aperture of the SOS suspensions are 31.75 mm. Thus, there is sufficient beam stay clear at all suspended optics, even

Table 8: Suspension design parameters for the 40m prototype upgrade.

Parameter	ETM	ITM	BS	PRM	SRM	MCC	MCF1	MCF2
Pendulum freq. (Hz)	.800	.800	1.000	1.000	1.000	1.000	1.000	1.000
Pitch freq., (Hz)	.500	.500	.744	.744	.744	.744	.744	.744
Yaw freq., (Hz)	.600	.600	.856	.856	.856	.856	.856	.856
Violin freq., (Hz)	451	459	641	628	628	645	645	645
Vertical freq. (Hz)	11.79	11.59	16.23	16.57	16.57	16.12	16.12	16.12
d(pendulum) (cm)	38.80	38.80	24.80	24.8	24.8	24.80	24.80	24.80
d(pitch) (cm)	.1195	.1195	.09	.09	.09	.09	.09	.09
d(yaw) (cm)	2.13	2.13	1.57	1.57	1.57	1.57	1.57	1.57
d(standoff) (mm)	1.00	1.00	1.00	1.00	1.00	1.00	1.00	1.00
d(margin) (mm)	.577	.577	.818	.818	.818	.818	.818	.818
wire dia (in)	.0036	.0036	.0017	.0017	.0017	.0017	.0017	.0017
susp height (mm)	425	425	417	417	417	417	417	417
susp transv. width (mm)	241	241	155	155	155	155	155	155
susp long. width (mm)	165	165	127	127	127	127	127	127
optic center height (mm)	140	140	140	140	140	140	140	140
optic dia (mm)	125	125	75	75	75	75	75	75
optic thickness (mm)	50	50	25	25	25	25	25	25
mass (kg)	1.276	1.320	.235	.225	.225	.238	.238	.238
wedge (deg)	2.5	1.0	1.0(s)	2.5	2.5	0.5	0.5(s)	0.5(s)
wedge orientation	left	right	right	right	left	left	right	left

the BS at 45°. Just to make sure, Material has been removed from the sensor/actuator brackets to increase the size of the aperture on all small optic suspensions.

The design parameters for all suspensions are summarized in Table 8. For more detail, see Ref. [39].

9.2 Suspension control

The suspension controllers for Initial LIGO [50] provide local velocity damping of the mirror motion, using information from the LED/PD pairs in the 5 OSEMs on each mirror optic, and/or information from optical levers viewing each mirror optic. Input from the global length and alignment sensing systems allow the mirror optics to be positioned at DC.

The Initial LIGO suspension controls have been redesigned [51] so that all feedback (local damping, and global control) is handled digitally.

This system is being essentially replicated for the 40m IFO, including all 10 suspended optics. Its ability to satisfy the design requirements is currently under study.

A preliminary (but pedagogically useful) design is presented in [31].

10 Control Electronics and photoelectronics

One of the primary motivations for the 40m upgrade is to spur the development of, and test the efficacy and robustness of, the control electronics. This includes:

- The ability to sense and control all five length degrees of freedom (the LSC system).
- The ability to sense and control all 7x2 angular degrees of freedom (the ASC system).
- The ability to use double-demodulation to sense some of the length degrees of freedom.
- The ability to maintain a detuned signal cavity (SRC).
- Establishing the expected response function for GW signals.
- The ability to offset-lock the arm cavities in order to allow a controlled amount of arm-filtered carrier light out the asymmetric port for DC GW sensing.
- The ability to sense the GW signal using DC sensing.

Although most of these functions require only a straightforward extension of the techniques already developed for Initial LIGO, further development is required, and the ability of all components to function as a coherent and robust system must be demonstrated.

Work required to design these systems is only just beginning.

As mentioned above in section 4.13, the CDS group currently believes that the architecture of the control, monitoring and data systems used in Initial LIGO (embedded VME processors running VxWorks and EPICS, and reflective memory modules with fiber links for the fast control, DAQS, and monitoring networks) will be adequate for Advanced LIGO as well. Thus, the 40m lab will be outfitted with a full complement of these control devices. The lab will have the infrastructure for maintaining all the embedded processors required for prototyping AdvLIGO, including fiber links to the “end stations” 40 meters away.

11 Input mode cleaner

A long suspended-mass mode cleaner would deliver a laser beam with LIGO-like beam quality (low frequency noise, low amplitude noise, low higher order mode HOM power, and low beam position and pointing jitter); this presumably will make lock acquisition and IFO operation less difficult and more LIGO-like, and increase the chances that fundamental noise sources can be exposed.

For control realism, we would like to have an input mode cleaner that is as similar to what is envisioned for Advanced LIGO as possible. Current thought is that an Advanced LIGO input mode cleaner could look very similar to the Initial LIGO 12m mode cleaner [52]; it might be increased to 16.7m in half-length in order to pass 9 MHz RF sidebands for control. As discussed in section 5.3, the 40m will operate with ~ 36 MHz sidebands, and a 12.7m mode cleaner is called for.

These considerations have led to a decision to construct a 12.7m suspended mass input mode cleaner for the 40m. A triangular 12m suspended-mass mode cleaner was designed for the 40m back in 1995, was partially built but never installed, and was subsequently disassembled. We have recovered three 4m long beam pipes, an end mirror chamber and seismic stack, and supports.

We have designed, constructed, and installed the additional hardware required to assemble the 12m input mode cleaner vacuum envelope. The vacuum equipment was cleaned and baked, and installed in the 40m vacuum envelope in the July of 2001.

In this section, we summarize the design of the 40m input mode cleaner. The only significant change with respect to the Initial LIGO design is a slightly different half-length, in order to fit into the existing mode cleaner vacuum tubes (in retrospect, this was entirely unnecessary, because the

Table 9: Design parameters for the input mode cleaner for the 40m prototype upgrade.

Parameter	Unit	Value
Plane mirror transmittance		$0.002 \pm 100\text{ppm}$
Plane mirror reflectance		$0.998 \pm 100\text{ppm}$
Curved mirror transmittance		$1\text{E-}05 +0, -10\text{ppm}$
Rear surface AR coating		$>99.8\% +0.2\%, -0$
Mirror absorbance/scattering each		<0.00010
Finesse		1550
Free spectral range	MHz	11.822
Pole frequency	kHz	3.818
Cavity full width/half max	kHz	7.63
Cavity full width/half max	nm	0.343
Cavity storage time	μs	42
Cavity optical half-length	mm	12680
Curved mirror radius of curvature	mm	$17869 +250, -350$
$g = 1 - L/R$		0.2904
waist size	mm	1.657
Raleigh range	m	8.111
Beam divergence	mrad	210
Transmission of 00 mode		0.976
1 ppm intensity, curved mirror	mm	16.2
100 ppm intensity, curved mirror	mm	13.2

tubes required redesign and were built anew). The optical layout of the mode cleaner is shown in Fig. 9.

The half-length of the mode cleaner is 12.68 m, giving a free spectral range (FSR) of $f_{MC} = 11.8$ MHz. All IFO-sensing sidebands are chosen to be multiples of FSR of the MC, so that they are transmitted with high efficiency; we thus choose $f_1 = 3f_{MC} = 35.5$ MHz and $f_2 = 5f_1 = 177.4$ MHz.

The parameters of the input mode cleaner are summarized in Table 9.

The expected performance of the input mode cleaner is summarized as follows:

- Rejection of frequency noise: the mode cleaner has a cavity pole of 3.8 kHz. Frequency noise at higher frequencies are filtered out, as illustrated in Fig. 10.
- Rejection of higher order (non- TEM_{00}) transverse modes (HOM's): the large Guoy phase difference in the MC cavity ($g \ll 1$) suppresses the resonance of HOM's. Fig. 11 shows the transmittances of the first 16 HOM's, as a function of the cavity g -factor. As in Initial LIGO, we choose a g -factor near the minimum at $g = 0.29$. This produces transmittances for the first 20 HOM's (TEM_{mn}), as a function of $m + n$, shown in Fig. 12.
- Rejection of laser position and direction jitter.

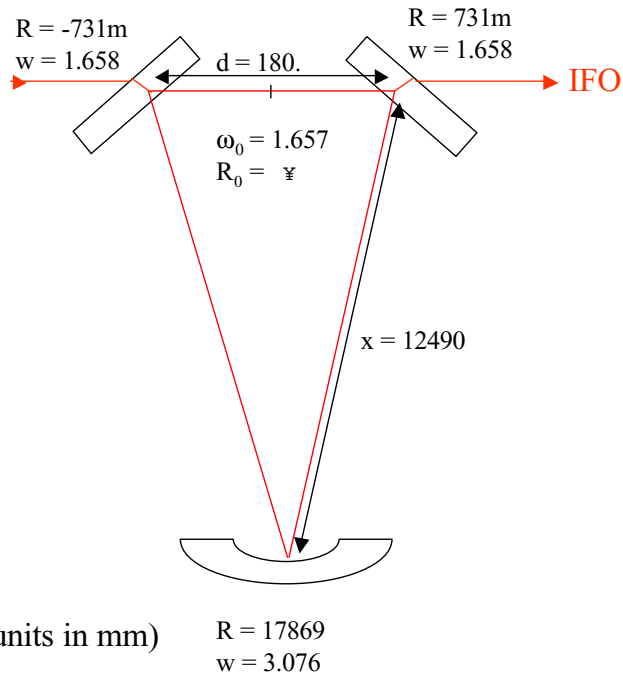


Figure 9: Layout of the 12m input mode cleaner for the 40m IFO.

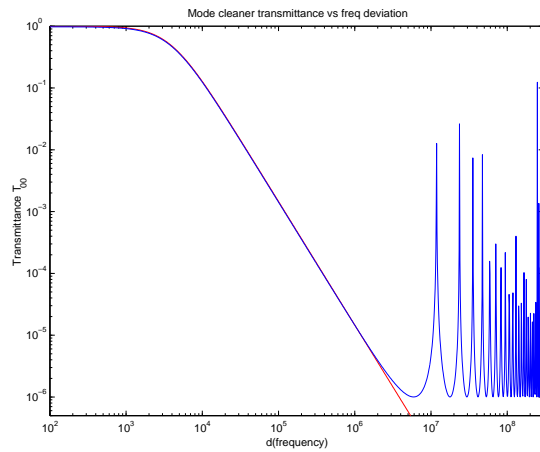


Figure 10: Calculated frequency response of the input mode cleaner transmission.

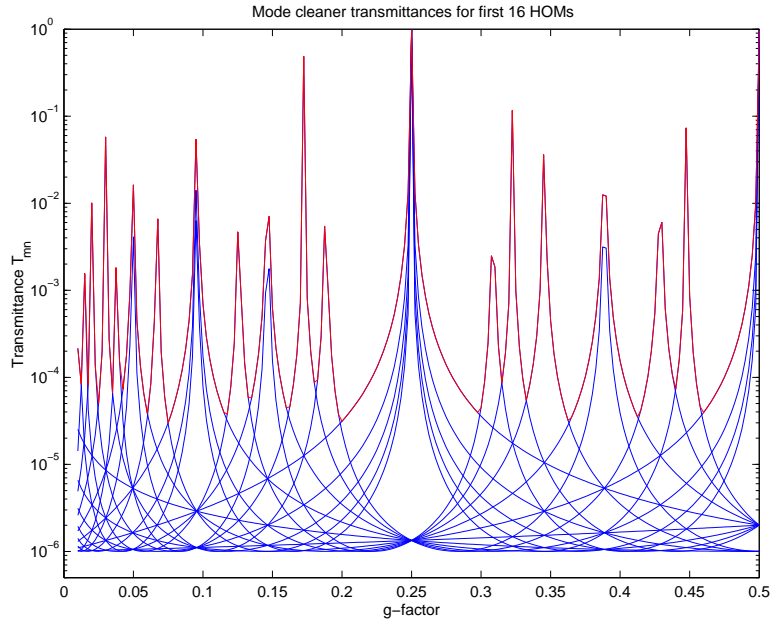


Figure 11: 12m input mode cleaner transmittances of the first 16 HOM's, as a function of the cavity g -factor. As in Initial LIGO, we choose a g -factor near the minimum at $g = 0.29$.

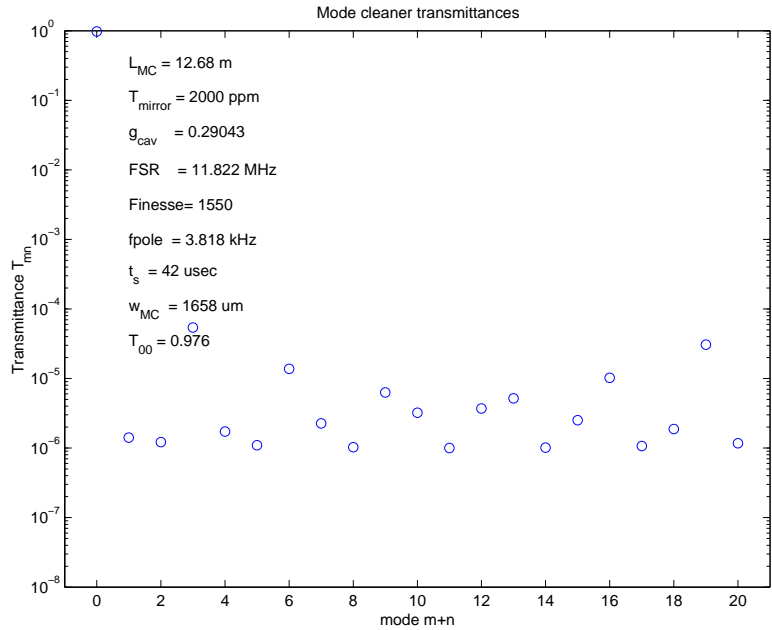


Figure 12: 12m input mode cleaner transmittances of the first 20 HOM's (TEM_{mn}) for a g -factor of $g = 0.29$, as a function of $m + n$.

12 Optical Layout

A detailed optical layout for the 40m dual-recycling interferometer, in AutoCAD, has been developed by Mike Smith see Fig. 13, and the details in Ref. [53].

The features of the layout include:

- All in-vacuum components laid out.
- Optical levers for all suspended masses.
- Camera views for all suspended masses.
- Baffling, scattered light suppression, shutters, *etc.*.
- Eleven output beams routed to optical tables near electronics racks.
- 12m Input mode cleaner, small monolithic output mode cleaner, mode-matching telescopes all designed and laid out.
- Detailed layouts of all in-vacuum optical tables, including all optical and electro-optical components, and a detailed parts list.
- Detailed layouts of all out-of-vacuum optical tables, including all optical and electro-optical components, and a detailed parts list.
- Integrated with building, electrical, CDS layout.

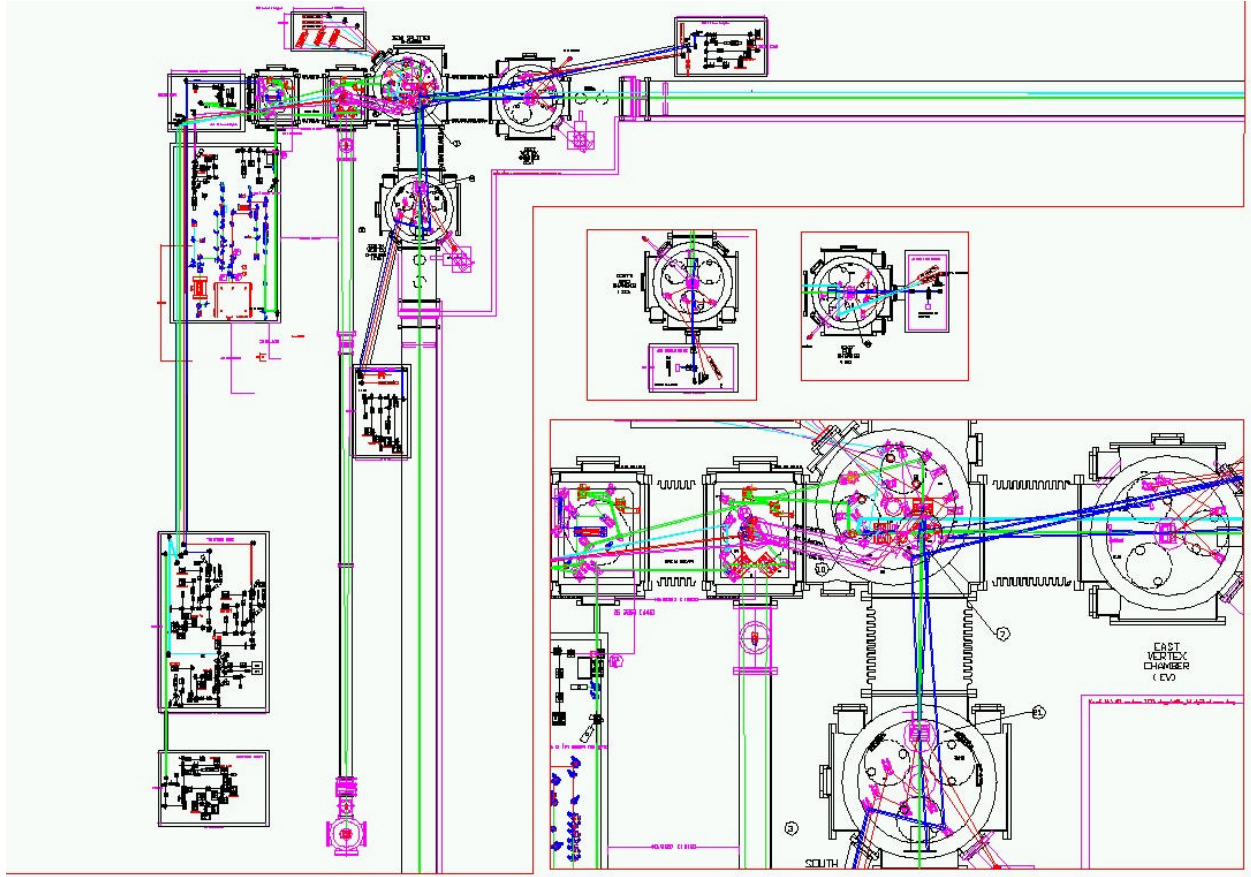


Figure 13: A view of the detailed integrated AutoCAD drawing of the 40m optomechanical, electrical, and building layout, by Mike Smith.

13 Noise

13.1 Fundamental noise at 40m

We can estimate the level of fundamental noise at the 40m; this is shown in Fig. 14, for an input laser power of 0.1 watts (to increase the shot noise so that it is larger than the test mass thermal noise).

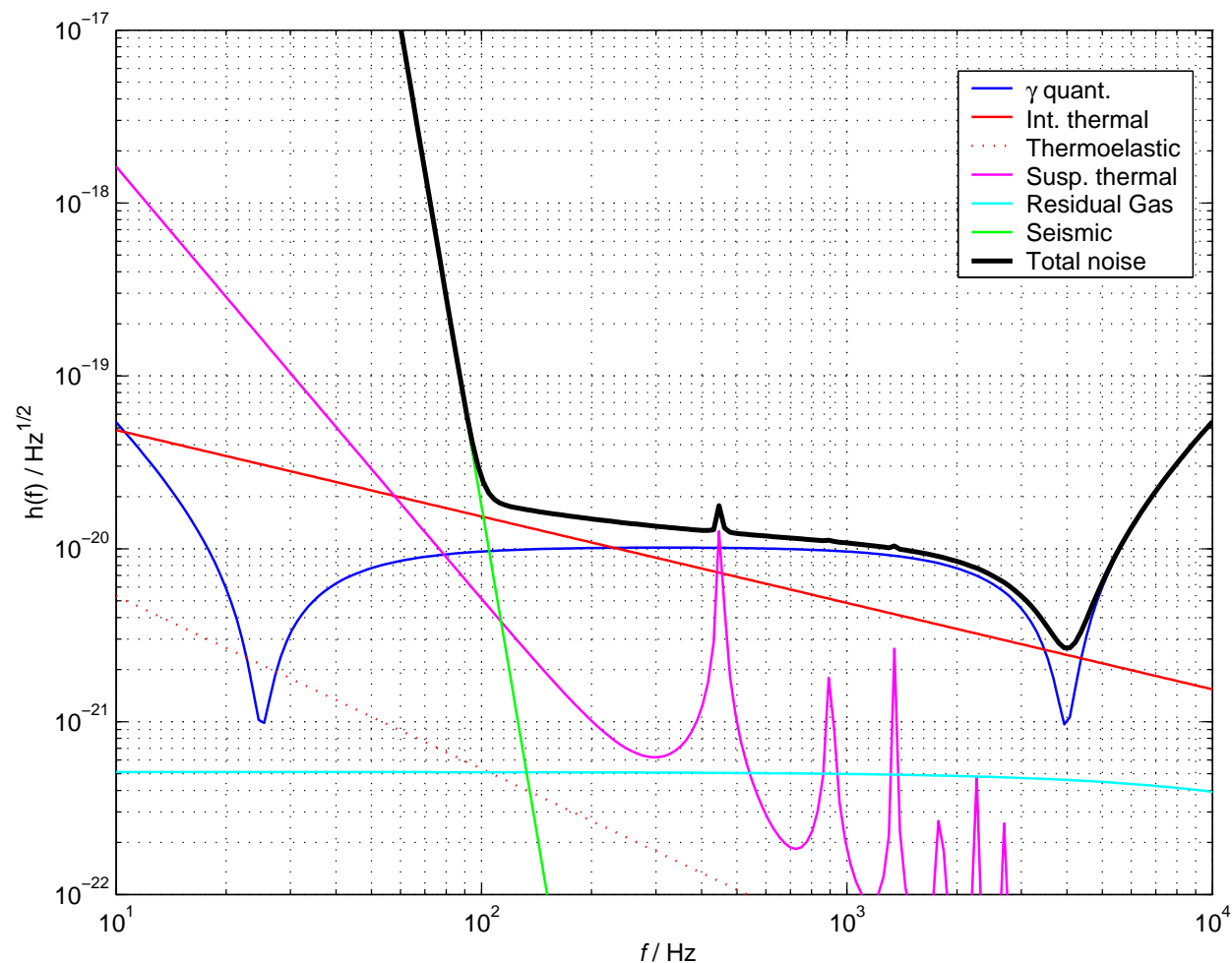


Figure 14: Estimate of fundamental noise at the 40m, for an input laser power of 0.1 watts.

Things to note:

- Below ~ 100 Hz, seismic noise dominates.
- From ~ 100 to ~ 200 Hz, the noise is dominated by the Brownian thermal noise of the test mass optics.
- Thermoelastic, and photothermal noise are negligible.
- Suspension noise is not very important. We may see a peak at the first violin resonance (at 450 Hz).

- The shot noise curve for 0.1 watt of input laser power, exhibiting a dip at the detuned frequency of 4000 Hz, lies above the test mass thermal noise for frequencies above ~ 250 Hz.
- At higher laser power (> 1 watt), the test mass thermal noise lies above the shot noise curve. If we want to expose the shot noise, especially in the dip region, we will need to turn the laser power down.
- Even if the shot noise curve is not exposed, we will be able to verify the GW response by measuring the IFO transfer function as the L_- degree of freedom is excited by the LIGO GDS system.
- If it turns out to be difficult to operate at low power, we can simply live with thermal noise and not bother to expose the shot noise; focus on *controls* problem (and the thermal noise problem).

13.2 Sensing noise

The quantum sensing noise (radiation pressure, photon shot noise, and their correlations) are computed in BENCH using the formulas from Buonanno and Chen [54]. One sees the characteristic double dip, due to the correlation between the radiation pressure and photon shot noise. Placing the signal recycling dip at 4 kHz (by detuning the signal recycling cavity) produces a corresponding dip at ~ 24 Hz, and radiation pressure is negligible throughout.

13.3 Internal thermal noise

BENCH uses the formulas from Bondu *et al.*, [44]. The masses have a diameter of 125 mm and thickness of 50 mm. The beam amplitude radii are 3.0 mm at the ITMs and 5.2 mm at the ETMs. We assume a mirror quality factor $Q = 3 \times 10^5$, including all attachments.

The thermoelastic noise is negligible, as expected for fused silica.

13.4 Suspension noise

Suspension noise was modeled assuming test masses 1.3 kg, suspension pendulum frequency of $f_{susp} = 0.8$ Hz, and a pendulum loss angle of $\phi = 3 \times 10^{-6}$ (constant).

The violin modes are at multiples of 450 Hz. The effective mass of the modes, and the loss factors, are taken from Ref. [55].

13.5 Gas pressure noise

Residual gas in the beam pipe produces a fluctuating index of refraction, and thus a fluctuating phase shift on the beam, resulting in sensing noise. The resulting noise power spectral density is given approximately by [56]

$$N_{\text{resid gas}}^2(f) = \sum_i \frac{8\rho_i\alpha_i^2}{Lv_iw_0} e^{-f/f_i},$$

where the sum is over different gas species; ρ_i is the number density of gas species in $1/m^3$; α is the molecular polarizability in m^3 ($\alpha = (n-1)/\rho_0$, where n is the index of the gas at STP and ρ_0 is the number density of the gas at STP); v_i is the mean velocity of gas species in m/s ($v = \sqrt{2k_B T N_A/A}$,

where N_A is Avogadro's number and A is the atomic number of the gas species); w_0 is the average beam radius (approximately 4 mm); and f_i is the characteristic frequency for that gas species passing through the beam ($f_i = 1/(2\pi w_0/v_i)$).

The 40m vacuum is currently dominated by H_2O (5×10^{-7} torr), N_2 (3×10^{-7} torr), and H_2 (1×10^{-7} torr).

13.6 Seismic noise

The seismic noise shown in Fig. 14 is a simple model with a DC level of 1×10^{-10} m, a corner frequency at 21 Hz, and a power-law falloff with exponent of -12.5. It nicely covers the expected (night-time) seismic noise at the mirrors, filtered through the active seismic isolation, passive seismic stacks, and pendulum.

The five existing core-optics chambers (BS, SV, SE, EV, EE) have 4-stage, 3-leg/stage seismic stacks, fitted with viton springs. We have installed STACIS seismic isolation systems under the four test mass seismic stacks [8].

We have measured the seismic noise in all three axes, at the 40m lab [7]: see Fig. 15. We have measured and compared the spectra between day and night: see Fig. 16. (V,H; day, night)

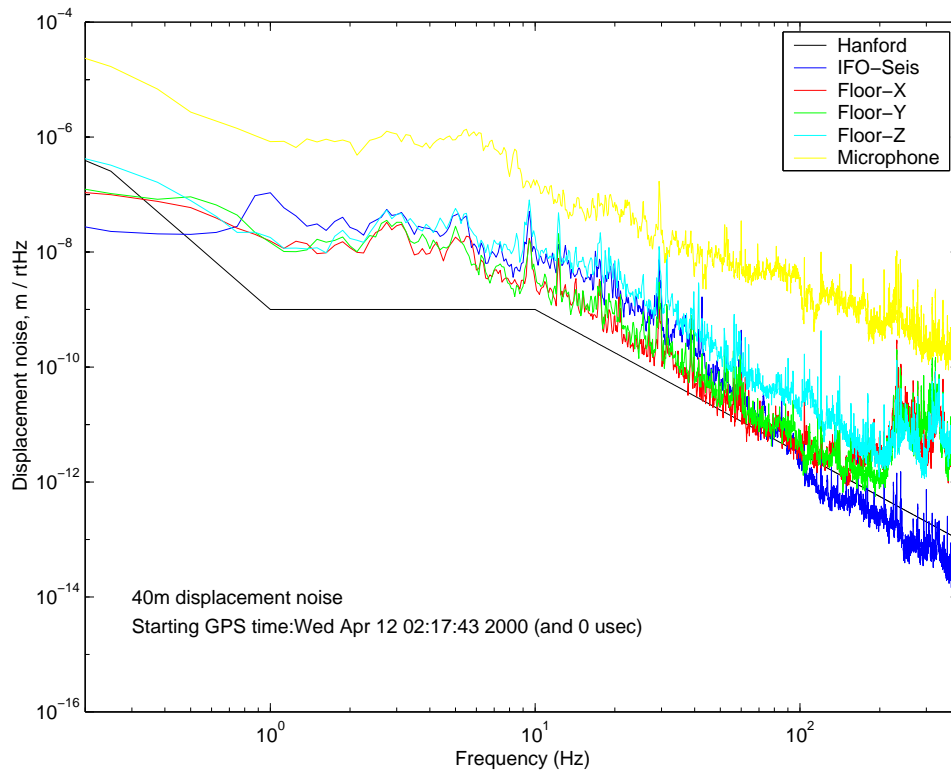


Figure 15: Seismic displacement noise spectra at the 40m lab during the day, in X , Y , Z (vertical). Solid line is the Hanford baseline displacement noise spectrum.

We can model the stack transfer functions and compare them with the attempts we've made to measure them with inadequate instrumentation. The vertical and horizontal transfer functions of the existing test mass stacks are shown in Fig. 17.

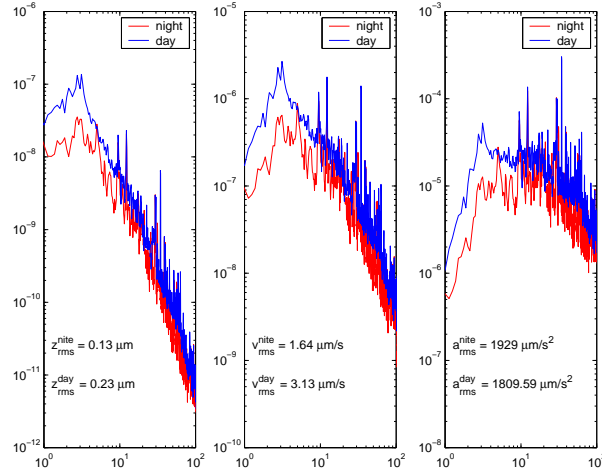


Figure 16: The (vertical) seismic displacement, velocity, and acceleration noise spectra at the 40m lab, comparing daytime with nighttime.

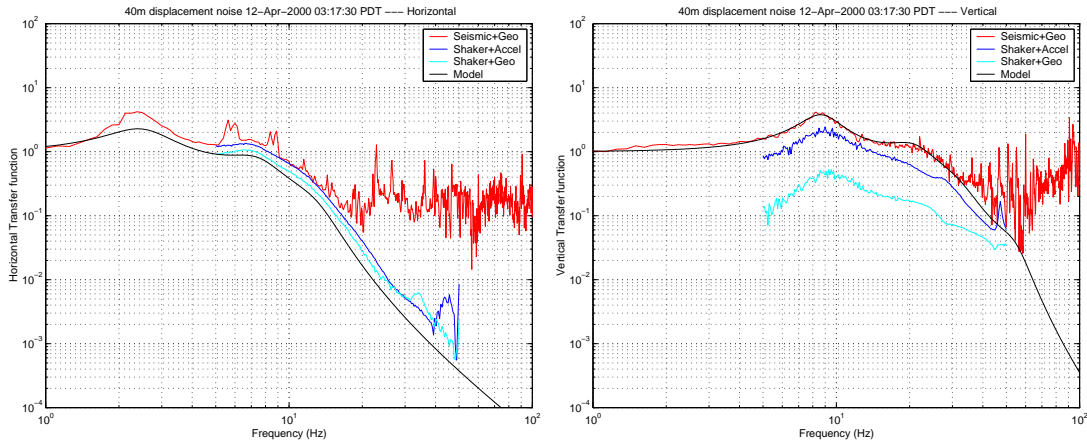


Figure 17: The horizontal (left) and vertical (right) transfer functions for the 40m test mass passive seismic stacks, as measured with various instruments, compared with a simple model (solid smooth line).

Finally, we can use the measured seismic spectrum, at the mirrors, filtered through the active seismic isolation, passive seismic stacks, and pendulum, to estimate the velocity noise spectrum at the test mass (with STACIS turned on). We can integrate to find the rms velocity of the test masses down to 0.1 Hz and 1.0 Hz. These are shown in Fig. 18.

Studies of lock acquisition [57, 29] show that the most critical parameter for acquiring lock is the rms velocity of the test mass, and that rms velocities $\ll \lambda/s$ are required.

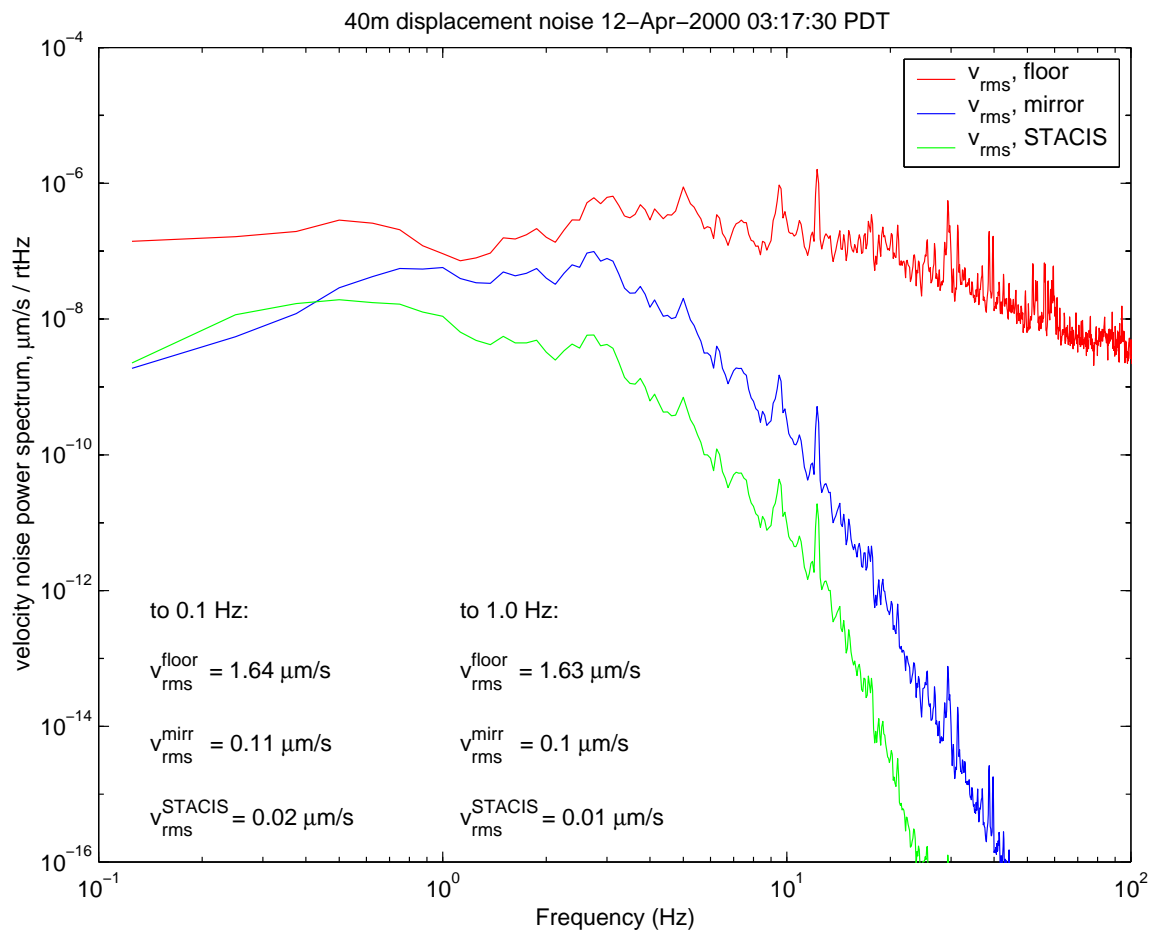


Figure 18: An estimate of the velocity noise spectrum (in $\mu\text{m/s}/\sqrt{\text{Hz}}$) of the floor (top, red trace), of the test mass with STACIS turned off (middle, blue trace), and of the test mass with STACIS turned on (bottom, green trace). Also shown are the derived rms velocities down to 0.1 Hz and 1.0 Hz.

14 Outstanding issues

Here is a list of outstanding issues and non-trivial development tasks required for the success of the 40m dual recycling experiment:

- Development of the servo electronics, and fast in-vacuum steering mirrors, for steering the PSL beam into the input mode cleaner, from the input mode cleaner into the core interferometer, and from the core interferometer into the output mode cleaner.
- Development of electro-optic modulators capable of operating at 180 MHz, with high-power beams, and large aperture. This is being pursued at U. Florida.
- Development of photodetectors capable of operating at 180 MHz, with high-power beams, and large aperture. Actually, for the 40m, we need demodulation at $180+36 = 216$ MHz.
- Development of wavefront sensors capable of operating at 180, or 216, MHz.
- Development of the servo filters for the core interferometer length sensing and control system.
- Development of the servo filters for the core interferometer alignment sensing and control system.
- Simulation of lock acquisition dynamics for the 40m and for Advanced LIGO.
- Development of lock acquisition control software for dual recycled interferometer.
- Development of a full suite of automated calibration software (for suspension controllers, LSC, ASC, etc).
- Development of a full suite of diagnostics software for lock acquisition, measurement of transfer functions, diagnosis of noise sources, *etc.*

15 Schedule, milestones

Some significant milestones that have been reached:

- 3Q00: Dismantling of old 40m IFO, distribution of surplus equipment
- 1Q01: Completion of 40m laboratory building rehab, power conditioners
- 1Q01: New CDS racks and cable trays
- 1Q01: New vacuum control system
- 1Q01: Installation of STACIS active seismic isolation system
- 2Q01: New computers and networking for online
- 2Q01: Installation and commissioning of new DAQS system
- 2Q01: Installation of vacuum envelope for input mode cleaner
- 2Q01: All glass blanks for 10 suspended optics received (more spares on order).

- 2Q01: Glass blanks for mode cleaner optics, out for polishing
- 2Q01: Initial-LIGO SOS suspensions for MC, BS, RM, SM constructed
- 3Q01: Installation and commissioning of 10-watt laser and PSL
- 3Q01: Installation of new optical tables and supports
- 3Q01: Installation of PEM system and first round of instruments
- 3Q01: Completion of detailed in-vacuum optical layout
- 3Q01: Completion of detailed layout of out-of-vacuum interferometer sensing system

Significant milestones in the coming year:

- 3Q01: 40m dual recycling experiment conceptual design review
- 1Q02: All in-vacuum cables, feedthroughs, optical viewports, and last two seismic stacks installed
- 1Q02: Scaled suspensions for ITMs and ETMs constructed
- 1Q02: Optics for input mode cleaner polished and coated
- 2Q02: Optics for input mode cleaner suspended
- 2Q02: Digital suspension controllers for 10 suspended optics ready for commissioning
- 3Q02: Commissioning of input mode cleaner
- 3Q02: Acquisition of most of the electronics and photoelectronics for interferometer sensing and control (CDS, ISC, LSC, ASC)
- 4Q02: Core IFO Optics polished and coated
- 4Q02: Glasgow 10m experiment informs 40m program
- 4Q02: Control system finalized

Looking towards the experiments:

- 2Q03: auxiliary optics, IFO sensing and control systems assembled
- 3Q03: Core subsystems commissioned, begin experiments
Lock acquisition with all 5 length dof's, 2x6 angular dof's
measure transfer functions, noise
Inform CDS of required modifications
- 3Q04: Next round of experiments.
DC readout. Multiple pendulum suspensions?
Final reports to LIGO Lab; publications.

16 Appendix A - Acronyms

40m - The LIGO Caltech 40 Meter Interferometer Laboratory
BS - Beam splitter
CDS - LIGO Control and Data system
DAQS - LIGO data acquisition system
DR - Dual recycling
ETF - LIGO test interferometer facility at Stanford
ETM - End test mass
FSR - Free spectral range
IFO - Interferometer
IMC - Input mode cleaner
ITM - Input test mass
LASTI - LIGO test interferometer facility at MIT
MC - Mode cleaner
OMC - Output mode cleaner
PEM - LIGO physics environment monitoring system
PMC - LIGO PSL pre-mode cleaner
PNI - Phase noise interferometer at MIT
PR - Power recycling
PRC - Power recycling cavity
PRM - Power recycling mirror
PSL - LIGO pre-stabilized laser
R, r - power and amplitude reflectivity through a mirror or optical system
ROC - radius of curvature
RSE - Resonant sideband extraction
SEI - LIGO seismic isolation system
SR - Signal recycling
SRC - Signal recycling cavity
SRM - Signal recycling mirror
SUS - LIGO suspension system
T, t - power and amplitude transmission through a mirror or optical system
TNI - Thermal noise interferometer at Caltech

17 Appendix B - Gaussian Beam Optics

For a linear Fabry-Perot optical cavity of length L , such as the IFO arms, we define [58, 59] a g-factor $g = g_1 g_2$, where $g_i = 1 - L/R_i$, $i = 1$ or 2 for the ITM or ETM, respectively, and R_i is the ROC of mirror i . Cavities with $g < 1$ are stable. Furthermore, it can be shown that with beam spot sizes w_i at the two mirrors, the value of $\sqrt{w_1^2 + w_2^2}$ is minimized with $g = 1/3$. We refer to this as optimal stability, and choose this value for the 40m arm cavities (as for the LIGO cavities).

For a symmetric cavity, we specify $g_1 = g_2 = \sqrt{g}$, while for a half-symmetric cavity, we specify $g_1 = 1$ (flat ITM) and $g_2 = g$.

The beam waist in such a cavity (field amplitude $1/e$ radius; power $1/e^2$ radius); is determined from the standard formulas:

$$w_0^2 = \frac{\lambda}{\pi} \frac{\sqrt{L(R_1 - L)(R_2 - L)(R_1 + R_2 - L)}}{R_1 + R_2 - 2L}.$$

Here, $\lambda = 1064$ nm.

The Rayleigh length of the beam is

$$z_R = \pi w_0^2 / \lambda.$$

For a half-symmetric cavity, this reduces to

$$w_0^2 = \frac{\lambda L}{\pi} \sqrt{\frac{g}{1-g}}, \quad \text{and} \quad z_R = L \sqrt{\frac{g}{1-g}}.$$

The distance of the waist to mirror 1 (the ITM) is

$$z_i = L(R_2 - L) / (R_1 + R_2 - 2L).$$

The width of the beam (field amplitude $1/e$ radius) at a distance z from the waist is

$$w(z) = w_0 \sqrt{1 + (z/z_R)^2}$$

and the radius of the beam wavefront there (which should match the ROC of a focussing optic, if any, there) is

$$R(z) = z + z_R^2 / z.$$

Note that at the waist, $R(0) = \infty$, and $w(0) = w_0$ is minimized. Far from the waist ($z \gg z_R$, ie, the geometrical optic limit), $R = z$ and $w = (w_0/z_R)z$. The power $1/e^2$ diameter is $d_{1/e^2} = 2\sqrt{2}w$, so that the beam divergence full-angle is

$$\theta = 2\sqrt{2}(w_0/z_R) = 2\sqrt{2}\lambda / (\pi w_0).$$

These equations define the beam in the F-P cavity. For LIGO-like IFOs, the arm cavities *define* the TEM₀₀ mode of the beam, and all upstream optics must match efficiently into the arms. Thus, one must propagate the beam in the arms upstream, determine the beam wavefront radius at the location of each optic, and choose that to be the ROC of the optic placed in that location (except for the BS, which is not a F-P focussing element).

We can use the above formulas to propagate the beam upstream, taking into account the focussing of the curved optics and the different optical path length through fused silica. It is easier, however, to do this using the complex beam parameter $q(z)$, where [59]

$$\frac{1}{q(z)} = \frac{1}{R(z)} - \frac{i\lambda}{\pi w^2(z)}.$$

This beam parameter can be propagated through empty space: $q(z_2) = q(z_1) + (z_2 - z_1)$; through a substrate of thickness t and index of refraction n : $q(z_2) = q(z_1) + t/n$; and through a thin focussing element (like a mirror surface of ROC R): $1/q(z_2) = 1/q(z_1) - 1/R$.

At any point, the beam parameters may be determined:

$$R(z) = \frac{1}{\text{Re}(1/q)}, \quad \text{and} \quad w(z) = \sqrt{\frac{-\lambda}{\pi \text{Im}(1/q)}}.$$

Optimal mode matching then requires any focussing optic placed at that point to have a $ROC = R(z)$.

Also at any point, the beam waist w_0 , and distance to the waist z_w , may be determined:

$$z_w = \text{Re}(q), \quad \text{and} \quad w_0 = \sqrt{\frac{-\lambda}{\pi \text{Im}(1/(q - z_w))}}.$$

Imperfect ROC for, eg, the recycling mirror will produce a beam that is not matched to the one defined by the arms (“mode mismatch”, MM). If this mismatch is small, and approximate expression for the fraction of power lost to higher order modes is [60]

$$MM = \left(\frac{w_0 - w_a}{w_a}\right)^2 + \left(\frac{z_w - z_a}{2z_R}\right)^2,$$

where w_0 is the beam waist of the incoming beam after passing through the imperfect optic, w_a is the waist of the beam defined in the arms, z_w is the distance to the waist for the incoming beam after passing through the imperfect optic, z_a is the distance to the waist of the beam defined in the arms, and z_R is the Rayleigh length of the beam defined in the arms. We want to keep $MM < 0.01$ everywhere.

A simple matlab program has been used to accomplish this propagation, and to evaluate the tolerances on the mirror ROC to keep $MM < 0.01$. They yield the numbers given in Table 7.

18 Appendix C - RSE, Signal Recycling, Dual Recycling

18.1 Motivation

Initial LIGO interferometer performance is effectively governed by one parameter: the transmissivity of the ITM, T_{ITM} (or, equivalently, $r_I \equiv \sqrt{1 - T_{ITM}^2 - Loss}$). We assume that the reflectivity of the end test mass $r_E \equiv 1$. T_{ITM} governs the arm finesse, cavity gain (power available for sensing DL at $f=0$), the light storage time, and the cavity pole f_{arm} (and thus the GW bandwidth).

$$\begin{aligned} \text{Finesse} &= \frac{\pi \sqrt{r_I r_E}}{1 - r_I r_E}; \\ G_{arm} &= \left| \frac{t_I}{1 - r_I r_E} \right|^2; \\ \tau_{arm} &= \frac{L_{arm}}{c} \frac{\sqrt{r_I r_E}}{1 - r_I r_E}; \\ 2\pi f_{polarm} &= \frac{1}{2\tau_{arm}}. \end{aligned}$$

As T_{ITM} is decreased, G_{arm} is increased, the light storage time is increased, and the arm cavity pole frequency $f_{pol-arm}$ and thus the GW detection bandwidth, is decreased.

Further, as the arm gain G_{arm} increases, the losses in the arms increase, and the michelson reflectivity thus decreases. The power recycling mirror reflectivity must also decrease to optimially couple the laser light into the IFO; thus, the power recycling cavity gain G_{prc} decreases. The product $G_{arm}G_{prc}$ remains roughly constant even as T_{ITM} , and thus G_{arm} and G_{PRC} individually, change.

From Mizuno’s sensitivity “theorem” [24], the peak sensitivity to gravitational waves can be written

$$h_0 \gtrsim \sqrt{\frac{2\hbar\lambda}{\pi c} \frac{\Delta f_{BW}}{G_{arm}G_{prc}P_{laser}}},$$

where Δf_{BW} is the bandwidth of the detector (roughly given by the arm pole frequency, $f_{polearm}$).

This is illustrated, for the 40m, by the busy plot in Fig. 19. For Initial LIGO, the one parameter T_{ITM} governs both the peak sensitivity (which is at DC) and the bandwidth, as illustrated in the top figure of Fig. 20. Note that LIGO I operates with: $T_{ITM} = 0.03$, Finesse = 204, $\tau_s = 1734$ usec, $f_{pole} = 91$ Hz, $G_{arm} = 130$, $G_{prc} = 60$, $h_{shot}(0) = 7.4e-24$.

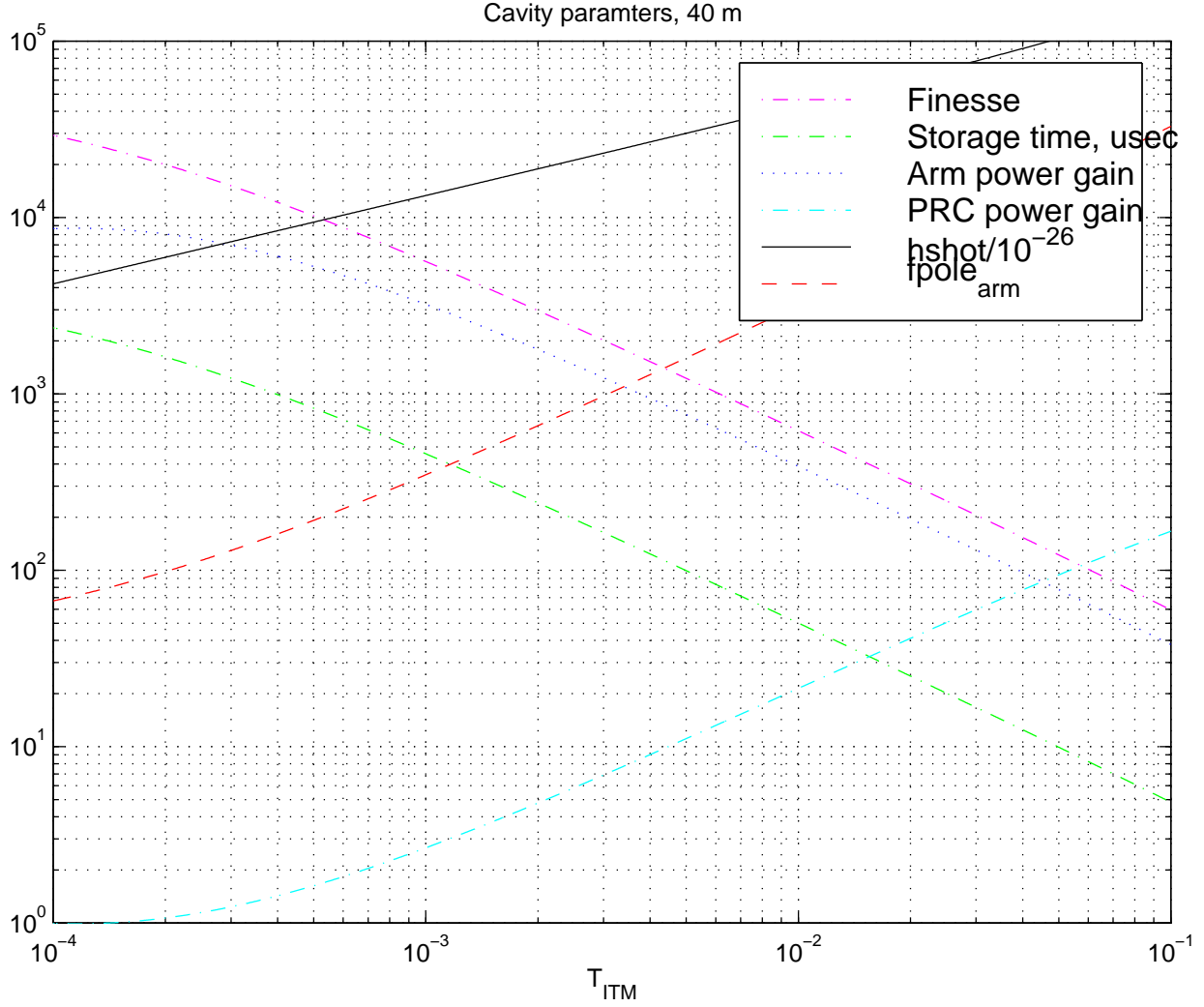


Figure 19: The arm cavity finesse F , the arm cavity storage time τ_s , the arm cavity pole frequency f_{pole} , the arm cavity power gain G_{arm} , the PRC power gain G_{prc} , the product $\sqrt{G_{arm}G_{prc}}$, and the DC shot noise strain sensitivity $h_{shot}(0)$, etc. as a function of the ITM transmissivity T_{ITM} .

Given all the other noise sources (seismic, thermal), which tend to be large at low frequencies, one optimizes the interferometer by choosing T_{ITM} to maximize sensitivity to binary inspirals, which have an $f^{-7/6}$ amplitude spectrum.

In practice, one “wastes” lots of photons at low frequency (near DC), where other noise sources dominate; we are wasting sensitivity at low frequencies.

We need the ability to optimize $h(f = 0)$ and f_{pol} independently, and sacrifice sensitivity at DC (where we are dominated by other noise sources) to improve sensitivity at higher frequencies where other noise sources are smaller (wider bandwidth).

The addition of one (or more) mirrors at the asymmetric port (signal recycling or RSE) allows one to independently optimize $h(f = 0)$ and f_{pol} ; by independently controlling the arm cavity gain for the carrier and for the signal sidebands (audio frequencies of GW signal). This then allows one to improve (typically, by a modest factor on the order of 2) the interferometer’s sensitivity to binary inspirals. This is illustrated in the bottom figure of Fig. 20.

This also permits a reduction of the gain in the PRC, where all the substrate material (BS, ITM) is; so if substrate losses dominate (over coating losses), or if substrate absorption leads to unacceptable heating and thermal lensing of the ITMs, signal recycling can help by allowing one to increase the gain of the arms, with concomittant decrease in gain of the PRC, while keeping the GW bandwidth large.

This signal mirror forms a cavity with the rest of the interferometer, called the signal recycling cavity (SRC) or signal extraction cavity (SEC). Depending on the tune of the carrier in the SRC (that is, the length of the cavity modulo one carrier wavelength λ), this mirror can modify the shot noise response in several ways [24, 33]:

- If the carrier is resonant in the SRC, the signal sidebands are resonantly extracted from the arms (resonant sideband extraction, or RSE), broadening the bandwidth of the detector relative to the inverse storage time of the carrier in the arms.
- If the carrier is anti-resonant in the SRC, the signal sidebands are sent back in to the interferometer to build them up (signal recycling or SR); this narrows the bandwidth of the detector and improves the DC shot noise $h(f = 0)$.
- If the carrier is neither resonant nor anti-resonant, but the signal sideband at some frequency f_{peak} is resonant, the transfer function will have a maximum there and the shot noise sensitivity will dip there.
- The reflectivity of the signal mirror (SM) governs the sharpness of that dip. The dip can be broad, to hug the thermal noise curve (Fig. 20). Or, the dip can be narrow, to maximize sensitivity to narrow-band sources like pulsars (narrow banding).

An additional *possible* benefit of the signal mirror is wavefront healing. Since the power recycling cavity is degenerate, both TEM_{00} and higher order mode (HOM) light (generated by imperfect optics and misalignments) will resonate there (whereas only TEM_{00} carrier light resonates in the arms and is thus sensitive to gravitational waves). The signal mirror sends the “wasted” HOM light back into the interferometer, allowing it to “re-integrate” itself among the stored resonant light in the arms. This idea was explored by Bochner [30]. who found that it is a rather modest effect.

18.2 Dual recycling

The combination of power recycling (PR) and signal recycling (SR) is referred to as Dual recycling (DR). A simple realization of dual recycling, with minimal modification to the LIGO-I optical configuration, is shown in Fig. 21: a power-recycled Michelson IFO with Fabry-Perot arms, with a signal recycling mirror (SM) for resonant sideband extraction (RSE).

We have two nearly-identical Fabry-Perot (FP) arms, a power recycling cavity (PRC), and, with the addition of one more mirror at the dark port, a signal recycling cavity (SRC).

18.3 Coupled cavities

For the purposes of analyzing the PRC or SRC, we can imagine that the beam splitter (BS) plus arms can be folded together, thus represented by a single FP arm (this simplified representation of course requires modification when considering the Schnupp asymmetry). The addition of the PRC or the SRC can then be analyzed as a coupled cavity, as in Fig. 22. Light exiting from the orthogonal direction (*e.g.*, when analyzing the PRC plus arms, light exiting the dark port) can be thought of as a loss.

Note the sign convention for the reflected light in Fig. 22.

18.4 RSE

The signal recycling mirror (SM) at the dark port sees no carrier light (if the contrast is perfect), unless there is a gravity wave signal. We can think of the latter as signal sidebands on the carrier, at acoustic frequencies. The signal sidebands in the arms exit to the dark port through the ITM plus SM, seen as a compound mirror, with reflectivity

$$r_{cm}(\phi) = r_{ITM} - \frac{t_{ITM}^2 r_{SM} e^{-i\phi}}{1 - r_{ITM} r_{SM} e^{-i\phi}},$$

where $\phi = 2\pi\nu$ is the phase advance of the carrier plus GW signal, round trip in the SRC.

If the mirrors are held at resonance ($\phi = 0$), the transmission through the output cavity can be smaller than the ITM transmission by itself, so that the signal sidebands leak out the arms faster (resonant sideband extraction, RSE [24]).

Conversely, if the mirrors are held at anti-resonance, the transmission through the output cavity can be larger than the ITM transmission by itself, so that the signal sidebands are stored in the arms longer (signal recycling).

Thus, one can independently change the finesse (and therefore the storage time and IFO bandwidth) of the arms, for the gravity wave signal only, while leaving the finesse for the unmodulated carrier unchanged.

These considerations are illustrated in Fig. 23 and 24.

18.5 Initial LIGO, Advanced LIGO, and the 40m

Initial LIGO was optimized for maximum sensitivity to binary inspirals. Given the expected seismic and thermal noise limits, the parameters are: $T_{ITM} = 0.03$, Finesse = 205, $\tau_s = 1734 \mu\text{sec}$, $f_{pole} = 91$ Hz, $G_{arm} = 130$, $G_{prc} = 48$.

Given the expected seismic and thermal noise limits using active seismic isolation and sapphire test masses, the current optimized parameters call for $T_{ITM} = 0.005$, Finesse = 1231, $\tau_s = 10.5$ msec, $f_{pole} = 15$ Hz, $G_{arm} = 770$, $G_{prc} = 14$. The reduction in G_{prc} , in the presence of the larger laser power, reduces the effect of substrate absorption and thermal lensing. Then, the signal recycling is operated in a detuned-RSE regime, where the signal bandwidth is broadened.

At the 40m, we want to test the control scheme using the same cavity finesses / gains, since these are what determine the gains and bandwidths of the control loops while in lock. Choosing the same T_{ITM} as in Advanced LIGO, the 40m parameters are $T_{ITM} = 0.005$, Finesse = 1231, $\tau_s =$

99 μsec , $f_{pole} = 1591$ Hz, $G_{arm} = 770$, $G_{prc} = 14$. The much shorter arms means that the storage time is much shorter at the 40m, so the time-dependent dynamics of lock acquisition will, indeed, be different at the 40m than at LIGO (harder in some ways, easier in others).

Given the much larger f_{pole} at the 40m, we will want to use the signal cavity to narrow, not broaden, the bandwidth (by just a little bit); ie, we'll operate in the detuned-SR regime. This should have no impact on the control scheme, and thus no negative impact on the fidelity of the 40m prototype to Advanced LIGO.

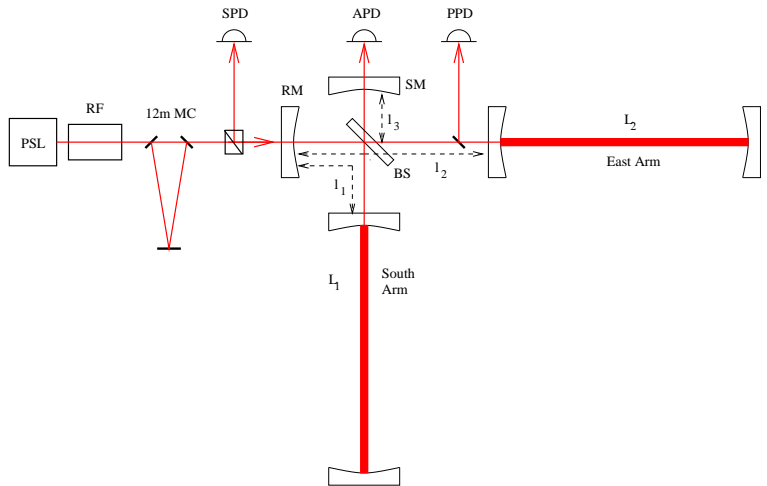


Figure 21: Configuration for a power-recycled Michelson IFO with Fabry-Perot arms, with a signal recycling mirror (SM) for resonant sideband extraction (RSE).

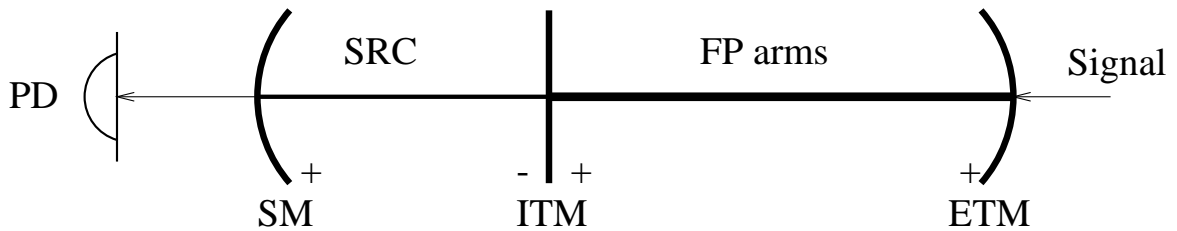


Figure 22: Simple model of signal-recycling IFO as a coupled cavity. Note the sign conventions for the reflected light for each mirror.

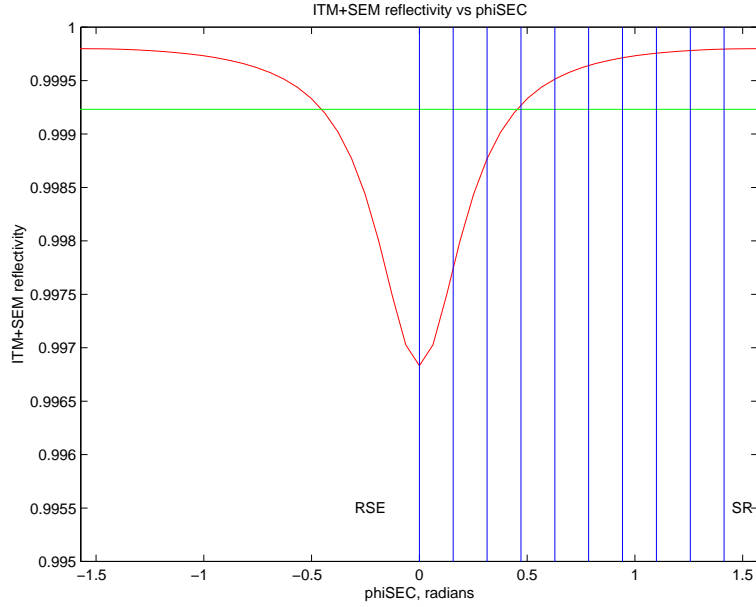


Figure 23: Amplitude reflectivity of the compound mirror formed by the ITM plus SM, for different detunings. The horizontal line is the ITM reflectivity. The vertical lines indicate detunings $\phi_{CS} = 2\pi\nu_{CS}$ in radians which correspond to the shot noise curves in Fig. 24.

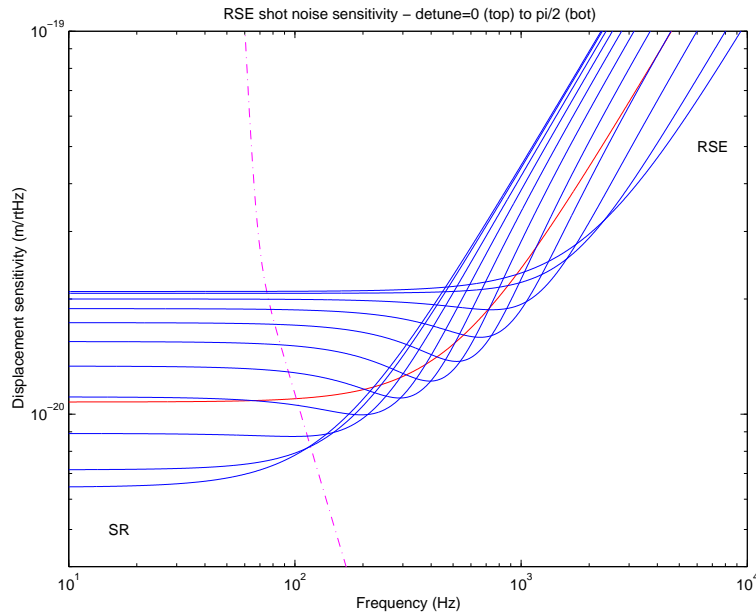


Figure 24: Shot noise displacement sensitivity versus GW frequency, for different SRC tunings. The middle, red curve, with no dip, corresponds to the absence of a SM; the other blue curves are in the presence of a SM, with tunes corresponding to the vertical lines in Fig. 23. They range from the narrow-band, $\phi_s = \pi/2$, “signal recycling” limit (bottom-most curve on the left), to the widest-band, $\phi_s = 0$, “resonant sideband extraction” limit.

19 Acknowledgements

Many thanks to Dennis Coyne, Gary Sanders, Barry Barish, Jim Mason, Bill Kells, Nergis Mavalvala, Ken Strain, Jay Heefner, Rolf Bork, Dale Ouimette, Alex Ivanov, Peter Fritschel, David Shoemaker, Mike Zucker, Daniel Sigg, Rai Weiss, Seiji Kawamura, Eric Gustafson, John Worden, Fred Raab, Jordan Camp, Phil Willems, Stan Whitcomb, Rick Savage, Dave Reitze, Dave Tanner, Riccardo DeSalvo, Szabi Marka, Ron Drever, Bill Althouse, Fred Asiri, Jenny Logan, Dick Gustafson, Keith Riles, Helena Armandula, Peter King, Lee Cardenas, Paul Russell, Todd Etzel, Eric Black, Shanti Rao, Ken Libbrecht, John Zweizig, Albert Lazzarini, Hiro Yamamoto, Biplab Bhawal, Ken Ganezer, George Jennings, Lisa Goggin, Ted Jou, Brian Kappus, Ivica Stefanovic, Richard George, Tim Piatenko, Andrea De Michele, Victor Tsai, Guillaume Michel, Larry Wallace, Lisa Bogue, Mike Pedraza, Tom Frey, Phil Lindquist, Florence Kaufman, Ed Chargois, Liz Wood, Rita Torres, Donna Tomlinson, Irena Petrac, ...

References

- [1] http://www.ligo.caltech.edu/~ajw/40m_upgrade.html
- [2] Plans for the 40m Upgrade, 5/21/99, LIGO G990132-00-D;
Optical Design Considerations for the 40m Upgrade, 10/6/99, LIGO G990133-00-D;
40m Upgrade Plans, 3/17/00, LIGO G990137-00-R;
40m Upgrade Plans, 5/1/00, LIGO G990134-00-R;
40 Meter Prototype Program - NSF Review, 1/18/01, G010009-00-R;
40 meter Prototype Program - LSC Meeting, 3/14/01, G010079-00-R;
Report to 40 Meter TAC, 8/13/01, G010281-00-R.
- [3] “Experimental demonstration of a suspended dual recycling interferometer for gravitational wave detection”, G. Heinzl *et al.*, Phys Rev Lett 81, 5493 (1998); and Phys Lett A 217, 305, (1996).
- [4] James Mason, PhD thesis, Caltech (2001).
Daniel Shaddock, PhD thesis, Australian National University (2000).
Thomas Delker, PhD thesis, University of Florida (2001), LIGO G000275-00.
S. Kentaro, University of Tokyo, LIGO G000277-00.
- [5] “Advanced LIGO Systems Design”, LIGO Scientific Collaboration, ed. P Fritschel, LIGO-T010075-00-D (2001). “Optical Layout for Advanced LIGO”, D. Coyne, LIGO-T010076-01-D (2001).
- [6] Upgrade of the 40m Vacuum System. LIGO note T000054-00-R (2000).
- [7] Measurement of Seismic Motion at 40m and Transfer Function of Seismic Stacks LIGO note T000058-00-R (2000).
- [8] “Performance of STACIS seismic isolation system at the 40 Meter Lab”, L. Jones, D. Ugolini, S. Vass, A. Weinstein, LIGO T010028-00-R (2000), draft obtainable from http://www.ligo.caltech.edu/~ajw/40m_stacis.html. See also “Performance of the Barry Controls, Inc STACIS active isolation system”, P. Fritschel and G. Gonzalez, LIGO-T950046-00-R, 1995; and <http://www.techmfg.com/Products/Advanced/STACIS2000.htm> .

- [9] “Proposal for Reorganization of 40m Computing”, A. Weinstein and D. Ugolini, LIGO note T000057-00-R (2000).
- [10] “Time Capsule at 40m Laboratory”, LIGO G000179-00-R, 07/31/2000.
- [11] LIGO drawings 1205425-1205429, 1205431-1205433, 1205435-1205439, 1205441-1205452, 1202092, 1101012.
- [12] J. Giaime, PhD thesis, MIT (1995); J. Giaime, P. Saha, D. Shoemaker, and L. Sievers, Rev. Sci. Instrum. 67, 208-214 (1996).
- [13] “Transfer function and drift measurements on the first-article HAM”, M. Barton, J. Giaime, G. Gonzalez, W. Johnson, A. Marin. LIGO-T980084-00, 10/98.
- [14] E. Ponslet, HYTEC-TN-LIGO-01 (1996); HYTEC-TN-LIGO-02 (1996); HYTEC-TN-LIGO-03 (1996); HYTEC-TN-LIGO-04a (1996); HYTEC-TN-LIGO-07a (1997);
- [15] Proposal for Upgrade of 40m Prototype - Large Seismic Stacks, and Bakeout, LIGO note T000055-00-R.
- [16] Partha Saha, Ph.D thesis, LIGO-P970012-00-R, MIT, February 1997.
- [17] J. Camp, D. Coyne, and D. Li, Appl. Opt. 38, 5378 (1999), LIGO P990032-00-D.
- [18] “Vacuum Pressure at the 40 Meter and the New Output Optic Chamber”, A. Weinstein, S. Vass, D. Ugolini, LIGO note T000126-00-R (2000).
- [19] “Standard Operating Procedure LIGO 10-W Laser for the Interferometer Operating in the Caltech 40 Meter Laboratory”, A. Weinstein and P. King, LIGO M010088-00-R (2000).
- [20] “LIGO Laser Safety Program”, LIGO-M960001-B-P (1996).
- [21] “Sensing and Control for LIGO II - LSC Meeting at Hanford, August 15-17, 2000”, Peter Fritschel and Ken Strain, LIGO G000225-00-D (8/15/2000).
- [22] “Science Benchmarks for Interferometer Trade Studies”, L.S. Finn, LIGO T970167 (1997); <http://gravity.phys.psu.edu/~lsf/Benchmarks/>.
- [23] “Calculation of Cavity Lengths and RF Frequencies for RSE at the 40M”, A. Weinstein, LIGO note T000056-00-R (2000).
- [24] “Comparison of optical configurations for laser interferometric gravitational wave detectors”, Jun Mizuno, PhD thesis, Max Plank Institut für Quantumoptik, July 1995.
- [25] “Pre-Stabilized Laser (PSL) Conceptual Design”, R. Abbott, P. King, R. Savage, S. Seel, LIGO T970087-04-D (1997). “Pre-stabilized Laser (PSL) Final Design Document”, R. Abbott, P. King, LIGO T990025-00-D (1999).
- [26] “Twiddle (ver. 3.0) - A Program for Analyzing Interferometer Frequency Response (Mathematica 3.0)”, J. Mason, M. Regehr, H. Yamamoto, LIGO note T990022 (1999). Includes recent updates by J. Mason.

- [27] “Principles of Calculating the Dynamical Response of Misaligned Complex Resonant Optical Interferometers”, Daniel Sigg and Nergis Mavalvala, LIGO P990005-C-D (2000).
- [28] “End to End Simulation Program for Gravitational-Wave Detectors”, H. Yamamoto *et al.*, LIGO P000018-00-E (2000); “Overview of End to End Simulation Program”, LIGO Note T970193 (1997); <http://www.ligo.caltech.edu/~e2e/>
- [29] “Lock Acquisition of a Gravitational Wave Interferometer”, B. Bhawal *et al.*, LIGO-P010015-02-D (2001). “Han2k - End User’s Guide”, M. Evans *et al.*, LIGO T000094-01-E (2000). “Preliminary E2E-simulation studies of lock acquisition with misalignments”, Biplab Bhawal and Matt Evans, LIGO-T000106-00-E (2000).
- [30] “Modelling the Performance of Interferometric Gravitational Wave Detectors with Realistically Imperfect Optics”, B. Bochner, PhD Thesis, MIT (1998).
- [31] “Understanding the LIGO Optics Suspension Controller Electronics Design” Ivica Stevanovic and A. Weinstein, LIGO T000097 (2000).
- [32] Matlab code by Jim Mason, 1999 and 2000.
- [33] “Signal Extraction and Optical Design for an Advanced Gravitational Wave Interferometer”, James Mason, PhD thesis, Caltech, January 2001.
- [34] Melody; a Matlab model by Beausoleil, R.. LIGO note G010160-00-Z (2001); and <http://www.phys.ufl.edu/LIGO/LIGO/STAIC.html#2> .
- [35] “Calculation of Cavity Lengths and RF Frequencies for RSE at the 40M”, A. Weinstein, LIGO T000056 (2000). “Determining Lengths and Optical Parameters for Dual Recycling at the 40m LIGO Prototype”, Ted Jou and A. Weinstein, LIGO T000121 (2000).
- [36] “Wavefront Sensing for the 40m LIGO Prototype”, B. Kappus and A. Weinstein, LIGO T000123-00 (2000).
- [37] See for example LIGO G010119-00-Z (2001). California State University, Dominguez Hills. Contact Ken Ganezer, ganezer@csudh.edu. MOU: LIGO M010207-00-M (2001). Web site: <http://www.csudh.edu/neutrino>.
- [38] “Input Optics Final Design”, R. Adhikari *et al.*, LIGO-T980009 (1998).
- [39] “Small Optics Suspension Final Design (Mechanical System)”, Seiji Kawamura and Janeen Hazel, LIGO-T970135 (1997).
- [40] K. Strain *et al.*, Phys.Lett. 194, 124 (1994).
- [41] Program `testmass5.c` by Kent Blackburn, based on code from (JR Hutchinson, J. Appl. Mech., Vol. 47, pp 901-907, Dec. 1980. Effective mass calculation from Aaron Gillespie, PhD thesis, LIGO-P950006, 1995.
- [42] “Effect of Beamsplitter Vibration Resonance Excitation on the Optically Sensed Cavity Length”, D. Coyne, LIGO-T980029 (1998).
- [43] “Core Optics Components Conceptual Design”, B. Kells *et al.*, LIGO-T960016 (1996).

- [44] F. Bondu, P. Hello, JY. Vinet, Phys Lett A246, 227 (1998).
- [45] Stan Whitcomb, private communication, 8/20/00.
- [46] Private communications from Janeen Romie, Garilynn Billingsley, Dennis Coyne, Bill Kells, Stan Whitcomb, and others.
- [47] <http://www.ligo.caltech.edu/~ligo2/scripts/l2refdes.htm> .
- [48] “Advanced LIGO - Coating Development and Preliminary Production Specifications”, Helena Armandula, LIGO-E000487-00-D (2000).
- [49] <http://www.ligo.caltech.edu/~gari/40M/index.html>
- [50] “Large and Small Optic Suspension Electronics Final Design”, J. Heefner, T980043-00-C (1998); “Input Optics CDS Preliminary Design”, J. Heefner and D. Ouimette, T980040-00-C (1998).
- [51] “Digital LOS and SOS Control Systems For LIGO” J. Heefner and R. Bork, T000073-00-C (2000).
- [52] “Input Optics Final Design Document”, Rana Adhikari *et al.*, LIGO T980009-01-D (1998); “Input Optics Preliminary Design”, Rana Adhikari *et al.*, LIGO T970144-00-D (1997).
- [53] “40m Optical Systems and Sensing Design Requirements Document & Conceptual Design”, Mike Smith, LIGO T010117-00-D (2001).
- [54] A. Buonanno and Y. Chen, Class. Quant. Grav. 18, L95 (2001), and Phys. Rev. D6404, 2006 (2001).
- [55] “Notes on Anelastic Effects and Thermal Noise in Suspensions of Test Masses in Interferometric Gravitational-Wave Detectors”, C. Brif, LIGO T990041-00-R (1999).
- [56] Ancient LIGO notes by Stan Whitcomb and Rai Weiss.
- [57] “The BIG BOOK of LIGO Lock Acquisition Design”, B. Ware, LIGO-T-980666-00-D, 8/98.
- [58] “Lasers”, Seigman.
- [59] “Laser beams and resonators”, H. Kogelnik and T. Li, Applied Optics 5, 1550 (1966).
- [60] “Alignment of resonant optical cavities”, D. Anderson, Applied Optics 23, 2944 (1984).